

BCSJ Award Article

Synthesis, Structures, and Reactivity of Kinetically Stabilized Anthryldiphosphene Derivatives

Akihiro Tsurusaki,[1] Noriyoshi Nagahora,[1] Takahiro Sasamori,[1] Kazunari Matsuda,[1] Yoshihiko Kanemitsu,[1] Yasuaki Watanabe,[2] Yoshinobu Hosoi,[2] Yukio Furukawa,[2] and Norihiro Tokitoh*[1]

[1]Institute for Chemical Research, Kyoto University, Gokasho, Uji, Kyoto 611-0011

[2]Department of Chemistry, School of Science and Engineering, Waseda University, 3-4-1 Okubo, Shinjuku-ku, Tokyo 169-8555

Received November 12, 2009; E-mail: tokitoh@boc.kuicr.kyoto-u.ac.jp

The first stable anthryldiphosphenes, **1** and **2**, were synthesized by utilizing kinetic stabilization of 2,4,6-tris[bis(trimethylsilyl)methyl]phenyl (Tbt) and 2,6-bis[bis(trimethylsilyl)methyl]-4-[tris(trimethylsilyl)methyl]phenyl (Bbt) groups, and were characterized by spectroscopic and X-ray crystallographic analyses. The UV–visible spectroscopic data suggested the electronic communication between the anthryl moiety and the P=P unit. It was found that TbtP=P(9-Anth) (**1a**: 9-Anth = 9-anthryl) showed weak fluorescence in hexane solution. Furthermore, the reactivities of anthryldiphosphene **1** with a chromium complex, chalcogenation reagents, a diene, and electron-deficient olefins have been revealed.

The chemistry of low-coordinated compounds of heavier group 15 elements has been one of the most attractive areas in main group element chemistry[1] since the synthesis and isolation of the first stable diphosphene (Mes*P=PMes*, Mes* = 2,4,6-tri-*tert*-butylphenyl) by taking advantage of kinetic stabilization reported by Yoshifuji and his co-workers.[2] Nowadays, it has been demonstrated that heavier dipnictenes, double-bond compounds between heavier group 15 elements, can be synthesized by introduction of efficient steric protection groups even in the case of the heaviest element, bismuth.[1,3,4] Indeed, we have reported the synthesis of kinetically stabilized dipnictenes (ArE=E′Ar; E, E′ = P, Sb, and Bi) by taking advantage of extremely bulky substituents, 2,4,6-tris[bis(trimethylsilyl)methyl]phenyl (denoted as Tbt) and 2,6-bis[bis(trimethylsilyl)methyl]-4-[tris(trimethylsilyl)methyl]phenyl (denoted as Bbt) groups and revealed their chemical and physical properties,[4,5] while Power and his co-workers have reported the synthesis of a series of dipnictenes bearing bulky *m*-terphenyl groups.[3b]

It is well-known that the HOMO–LUMO gap of a diphosphene (P=P) is smaller than that of an azo-compound (N=N) due to the smaller overlap of 3p orbitals. Theoretical calculations suggest that the LUMO of a diphosphene is the antibonding P=P π^* orbital, while the HOMO or HOMO−1 are the bonding P=P π orbital or the phosphorus lone pair orbital (n_+), both of which are close in energy.[6] In fact, it was reported that the stable diphosphenes underwent ready chemical reduction to afford the corresponding anion radical species due to their low-lying π^* orbitals.[5b,5c,7] Consequently, there has been much attention paid to the construction of extended π-electron-conjugated systems bearing low-coordinated phosphorus atoms utilizing their small HOMO–LUMO gaps from the viewpoint of material science.[8,9] Unique properties of phosphaalkenes and diphosphenes bearing an electrochemically active unit, such as amine,[10] *p*-phenylene,[11] ferrocene,[12] alkynyl,[13] another diphosphene,[14] and thiophene[15] units, have been reported so far. In particular, Protasiewicz and his co-workers reported the synthesis and photochemical properties of the poly(*p*-phenylenephosphaalkene)s[11b,11c] and poly(*p*-phenylenediphosphene),[11c] so-called "phospha-PPVs," bearing conjugative P=C or P=P bonds. Poly(*p*-phenylenephosphaalkene)s exhibit unique fluorescence due to their π-conjugated P=C unit, whereas poly(*p*-phenylenediphosphene) shows no appreciable photoluminescence. Moreover, they demonstrated that the low-coordinated phosphorus center should electrochemically communicate with the extended π-conjugated systems based on the comparison between a series of phospha-PPV oligomers with carbon analogs.[9,11d] Fundamental studies on the properties of a π-electron-extended system containing a diphosphene unit, which should possess apparently smaller HOMO–LUMO energy gap than that of the phosphaalkene derivative, are interesting and important to open new chemistry for material science.

Published on the web April 29, 2010; doi:10.1246/bcsj.20090295

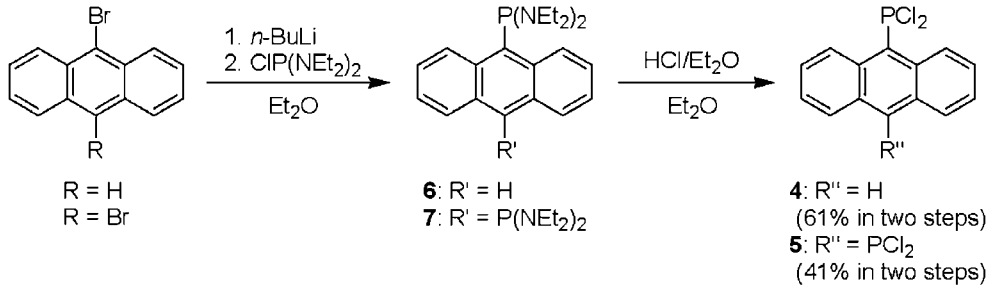

Scheme 1. Synthesis of **4** and **5**.

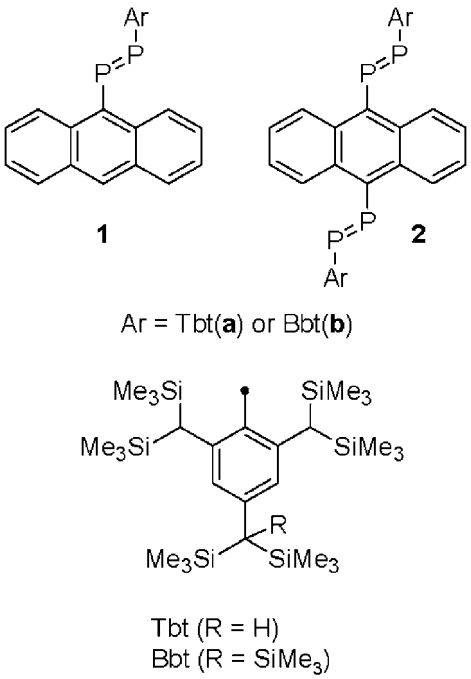

Figure 1.

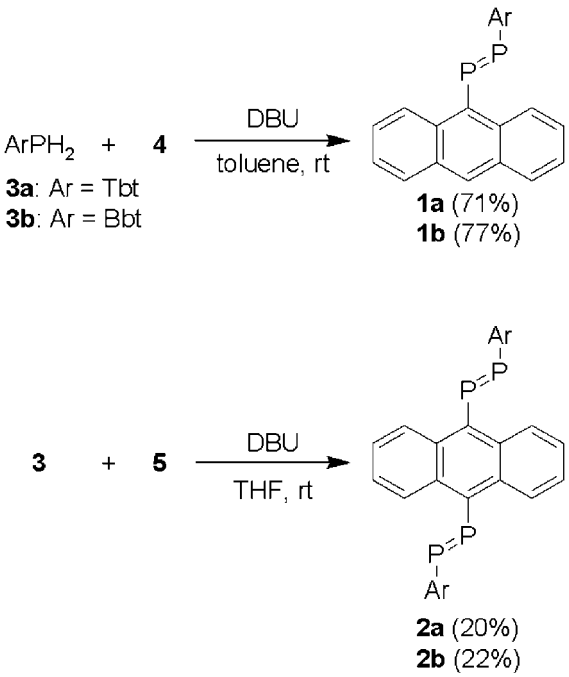

Scheme 2. Synthesis of **1** and **2**.

An anthryl unit is an interesting extended π-electron-conjugated system, since it has a simple aromatic structure bearing unique electrochemical and photochemical properties. Therefore, we have designed a 9-anthryldiphosphene, which has a diphosphene unit tethered with an anthracene moiety, as a novel π-conjugated diphosphene. Recently, we have preliminarily reported the synthesis of the first stable 9-anthryldiphosphenes **1** having Tbt (**1a**) or Bbt (**1b**) groups as an efficient steric protection group together with the structure and properties of **1a** (Figure 1).[16,17] We report here the details of the synthesis and properties of 9-anthryldiphosphenes **1** and more extended π-conjugated systems, 9,10-anthrylene-bridged bisdiphosphenes **2** (Figure 1). The reactivity of 9-anthryldiphosphenes **1** with a chromium complex, chalcogenation reagents,[18] a diene,[19] and electron-deficient olefins[19] is also described.

Results and Discussion

Synthesis of Kinetically Stabilized Anthryldiphosphenes 1 and 2. One of the most convenient methods for the synthesis of unsymmetrically substituted diphosphenes is a condensation reaction of a dihydrophosphine with a dichlorophosphine in the presence of a base.[20] 9-Anthryldichlorophosphine (**4**) and 9,10-bis(dichlorophosphino)anthracene (**5**) are readily prepared in moderate yields by the reactions of the corresponding lithiated anthracene derivatives with chlorobis(diethylamino)phosphine followed by the chlorination reaction using hydrogen chloride in diethyl ether (Scheme 1). Condensation reaction of $TbtPH_2$ (**3a**) and $BbtPH_2$ (**3b**) with 9-anthryldichlorophosphine (**4**) in the presence of DBU (DBU = 1,8-diazabicyclo[5.4.0]undec-7-ene) as a base afforded 9-anthryldiphosphenes **1a** and **1b** as stable red crystals in 71 and 77% yields, respectively (Scheme 2). 9,10-Anthrylene-bridged bisphosphenes **2a** and **2b** were also synthesized in ca. 20% yield in a manner similar to the synthesis of 9-anthryldiphosphenes **1a** and **1b** by using 9,10-bis(dichlorophosphino)anthracene (**5**) instead of 9-anthryldichlorophosphine (**4**).[21] The relatively low yields of **2a** and **2b** can be reasonably interpreted in terms of the decomposition of **5** in the presence of DBU. Exhaustive wash with hexane and recrystallization of the crude mixture from THF/hexane at $-40\,^{\circ}C$ afforded **2a** and **2b** in a pure form without any contamination of **3**.

The ^{31}P NMR spectra of **1** and **2** in C_6D_6 showed characteristic AB quartet signals at δ 526.2, 584.3 (**1a**), 521.9, 586.8 (**1b**), 528.8, 585.2 (**2a**), 522.1, 585.0 (**2b**), respectively, with $^1J_{PP} = 581–588$ Hz, supporting their P=P double-bond character similar to those of the previously reported unsymmetrically

substituted diaryldiphosphenes.[1a,22] The high-resolution mass spectra and elemental analysis also supported the structures of anthryldiphosphenes **1** and **2**.

Molecular Structures of Anthryldiphosphenes 1 and 2. The molecular structures of **1a**, **1b**, **2a**, and **2b** were revealed by X-ray crystallographic analysis. Some of them are depicted in Figures 2–4 and selected structural parameters are given in Tables 1 and 2. In both crystal packing diagrams of **1a** and **1b**, one can see the intermolecular π–π interaction (ca. 3.55 Å) between the anthryl moieties (Figure 2). Although the structural parameters of **1a** and **1b** are similar to each other, their packing structures are largely different in spite of the structural resemblance to their steric protection groups, Tbt and Bbt. That is, the anthryl moieties were found to be piled up along the *a* axis of the crystal lattice in the case of **1a** (Figure 2a), whereas the anthryl moieties of **1b** face each other in the center of the crystal lattice (Figure 2b). Surprisingly, the two different crystals of **2a** were obtained depending on the conditions of

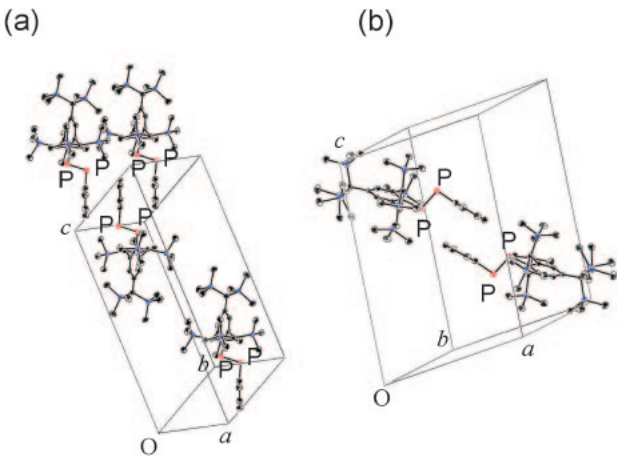

Figure 2. (a) Packing structure of **1a**. (b) Packing structure of **1b**.

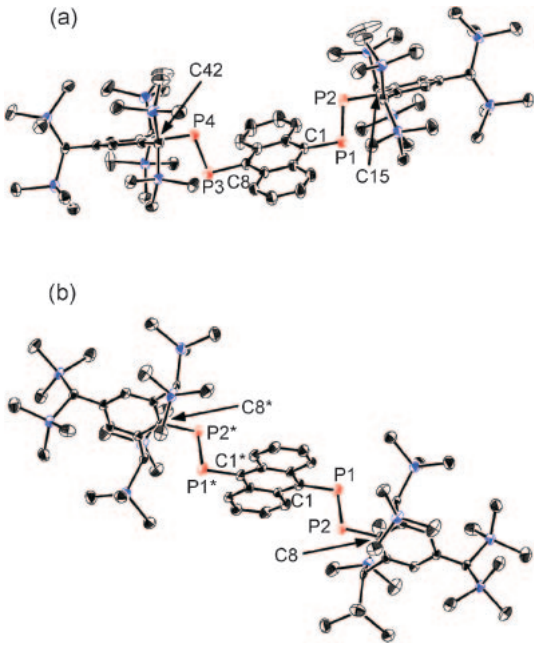

Figure 3. Molecular structures of (a) **[2a·toluene]** and (b) **[2a·2(benzene)]** with thermal ellipsoid plot (50% probability). Hydrogen atoms and solvated molecules are omitted for clarity.

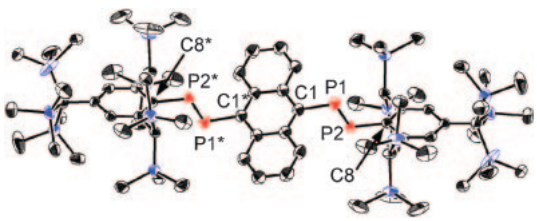

Figure 4. Molecular structure of **[2b·benzene]** with thermal ellipsoid plot (50% probability). Hydrogen atoms and a benzene molecule are omitted for clarity.

Table 1. Observed Structural Parameters for Diphosphenes **1** and **2**, a Diphosphene Chromium Complex **13**, and [4 + 2] Cycloadducts **31**

Compound	Bond lengths/Å			Bond angles/°		Ref.
	P–P	P–C(R)	P–C(Ar)	C(R)–P–P	C(Ar)–P–P	
1a	2.0352(16)	1.838(4)	1.848(4)	101.86(14)	100.79(13)	16
1b	2.0232(13)	1.842(3)	1.829(3)	97.66(11)	105.81(11)	17
[2a·toluene]	2.0274(12)	1.843(3)	1.846(3)	101.54(10)	99.90(10)	This work
	2.0374(11)	1.852(3)	1.842(3)	97.58(10)	102.57(9)	
[2a·2(benzene)]	2.0340(15)	1.849(4)	1.844(3)	97.83(13)	103.47(12)	This work
[2b·benzene]	2.0377(12)	1.855(3)	1.838(3)	100.38(10)	105.40(10)	This work
13	2.0307(10)	1.832(3)	1.847(3)	102.07(9)	109.23(9)	This work
[31a·1.5(benzene)]	2.0278(13)	1.895(3)	1.845(3)	102.98(11)	103.57(10)	17
[31b·3(benzene)]	2.022(2)	1.889(6)	1.834(6)	101.58(18)	105.43(19)	17
31c	2.0366(14)	1.903(4)	1.839(4)	100.34(12)	103.25(12)	17
[31d·1.5(benzene)]	2.0383(18)	1.896(4)	1.845(4)	103.17(15)	103.80(14)	17

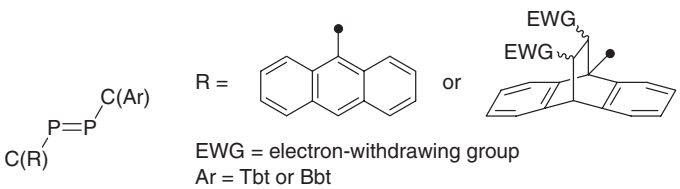

Table 2. Observed Dihedral Angles[a),b)] for Diphosphenes **1** and **2** and a Diphosphene Chromium Complex **13**

Compound	Dihedral angles/°	
	(CPP)–(Anth)[a)]	(CPP)–(Ar)[b)]
1a	81.65(10)	72.92(11)
1b	82.92(8)	80.44(10)
[2a·toluene]	76.66(8)	80.59(10)
	76.18(5)	78.64(9)
[2a·2(benzene)]	84.63(9)	76.68(12)
[2b·benzene]	83.38(6)	73.33(9)
13	84.65(6)	84.18(8)

a) Dihedral angles between the CPP plane containing 9-position of the anthryl group (Anth) and the anthryl moiety. b) Dihedral angles between the CPP plane containing the benzene ring *ipso*-carbon (Ar) and the benzene ring of the Tbt or Bbt groups.

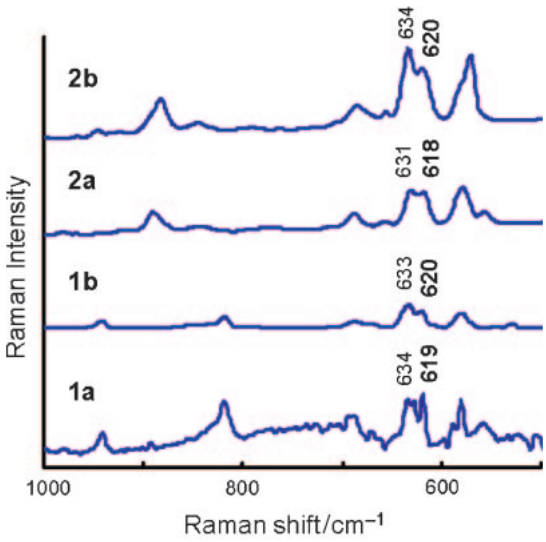

Figure 5. Raman spectra of **1a**, **1b**, **2a**, and **2b** described from bottom to top in order.

the crystal growth, where the two P=P units of **2a** were found to lie in the *syn*-configuration to the central anthryl moiety [recrystallization from its toluene solution at −40 °C (Figure 3a)] or in the *anti*-configuration [recrystallization from its THF/benzene solution at room temperature (Figure 3b)]. Recrystallization of **2b** from its THF/benzene solution at room temperature afforded single crystals, where it exhibits *anti*-configuration of the P=P unit as in the case of *anti*-**2a** (Figure 4). Structures of *anti*-**2a** and *anti*-**2b** possess the center of symmetry in the center of the anthryl moiety. Theoretical calculations for the real molecules of *syn*-**2a** and *anti*-**2a** performed at B3LYP/6-31G(d) level showed that s*yn*-**2a** is more stable than *anti*-**2a** by only 0.3 kcal mol^{-1} (1 kcal = 4.184 kJ), indicating the crystal packing force should be dominantly effective for the geometry of **2a**.[23]

The P=P bond lengths and P–P–C angles of **1a**, **1b**, **2a**, and **2b** are 2.0232(13)–2.0377(12) Å and 97.58(10)–105.81(11)°, respectively, which are similar to those for the previously reported diaryldiphosphenes (Table 1).[1a,4f] It should be noted that the dihedral angles between the central CPPC plane and the anthryl plane are 76.18(5)–84.63(9)°, indicating the less effective π-electron conjugation between the P=P and anthryl moieties in the solid state (Table 2).

Raman and Infrared Spectra of Anthryldiphosphenes 1 and 2. The double-bond characters of diphosphenes in the solid state can be characterized based on vibrational spectroscopy such as Raman spectroscopy.[4f,12h,24] The P=P stretching vibration of the previously reported diaryldiphosphenes were reported in the range from 603 to 622 cm^{-1},[4f,12h,24a,24b] the values of which are considerably higher than that of the diphosphane, Ph_2P–PPh_2, at 530 cm^{-1}.[25] The Raman spectra of **1a**, **1b**, **2a**, and **2b** are shown in Figure 5. Strong Raman lines were observed for **1a** and **1b** at 619, 634 (**1a**) and 620, 633 cm^{-1} (**1b**), respectively. The signals at 619 (**1a**) and 620 cm^{-1} (**1b**) are assignable to the corresponding P=P stretching frequencies on the basis of the estimated values of 612 cm^{-1} for the model compound of **1**, DmpP=P(9-Anth) (**8**; 9-Anth = 9-anthryl, Dmp = 2,6-dimethylphenyl).[26] The Raman spectra of **2a** and **2b** showed the two peak maxima at 618, 631 (**2a**) and 620, 634 cm^{-1} (**2b**), respectively, similar to those of anthryldiphosphene **1**. As in the case of monodiphosphene **1**, the signals at 618 (**2a**) and 620 cm^{-1} (**2b**) are assignable to the corresponding P=P stretching frequencies, the assignment of which were supported by theoretical calculations for the vibrational frequency of the real molecules, *syn*-**2a** (612 cm^{-1}) and *anti*-**2a** (611 cm^{-1}).[26]

Interestingly, bisdiphosphenes **2a** and **2b** were found to show their P=P stretching vibrational modes not only in the Raman spectra but also in the IR spectra.[12h] That is, the two types of vibration modes of the two P=P moieties should be conceivable for bisdiphosphenes **2a** and **2b** as in the same phase and the inverse phase. Theoretical calculations of *anti*-**2a** showed the P=P stretching vibrations in the same phase at 611 cm^{-1} (Raman active) and those in the inverse phase at 615 cm^{-1} (IR active), while theoretical calculations of *syn*-**2a** showed the inverse-phase vibrations at 612 cm^{-1} (Raman active) and the same-phase vibrations at 615 cm^{-1} (IR active).[26] In the IR spectra of **2a** and **2b**, the signals attributable to the P=P stretching vibrations were observed at 614 cm^{-1} (**2a**) and 616 cm^{-1} (**2b**), being in good agreement with the calculated value of real molecule **2a** (615 cm^{-1}).

Electrochemical Properties of the Stable Anthryldiphosphenes 1 and 2. The electrochemical properties of **1a**, **1b**, **2a**, and **2b** were furnished by cyclic voltammetry and differential pulse voltammetry, measurements of which were carried out in THF with *n*-Bu_4NBF_4 as an electrolyte at room temperature. Voltammograms of Bbt-substituted monodiphosphene **1b** and bisdiphosphene **2b** are shown in Figures 6 and 7, and the redox potentials of **1** and **2** are summarized in Table 3. Two reversible one-electron reduction couples were observed for **1a** and **1b** at $E_{1/2} = -1.73$, -2.32 (**1a**) and -1.66, -2.25 V (**1b**) versus Ag/Ag$^+$, respectively. It should be worthy of note that the first reduction potentials of **1** ($E_{1/2} = -1.73$ V for **1a** and -1.66 V for **1b**) at a less negative region than those of TbtP=PTbt ($E_{1/2} = -1.93$ V vs. Ag/Ag$^+$) and anthracene ($E_{1/2} = -2.42$ V vs. Ag/Ag$^+$) demonstrate the stability of the anion radical species of **1** probably due to the delocalization of the unpaired electron on the P=P and the anthryl moieties in solution. In addition, theoretical calculations for the electron

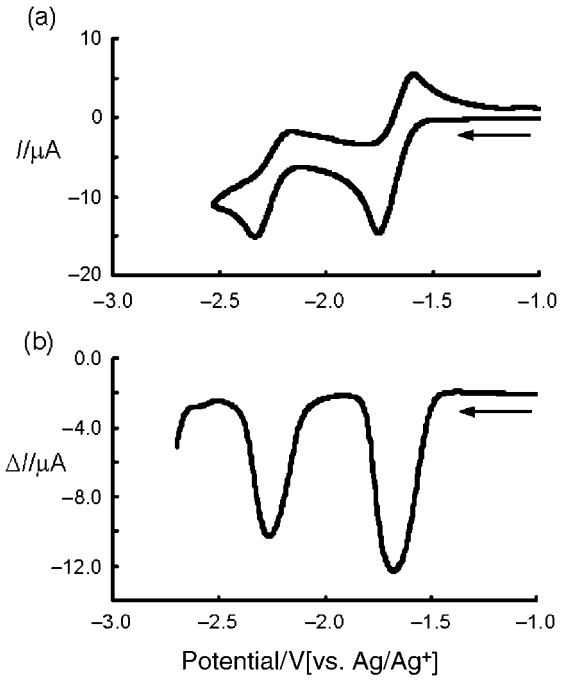

Figure 6. (a) Cyclic and (b) differential pulse voltammograms of **1b** in 0.1 M n-Bu_4NBF_4/THF solution at room temperature. $E_{1/2}(Cp_2Fe/Cp_2Fe^+) = +0.20$ V vs. Ag/Ag^+.

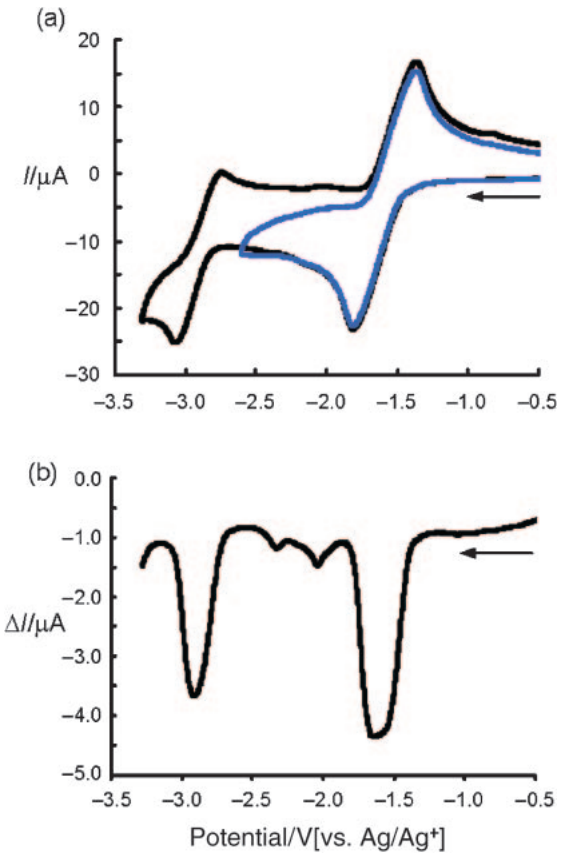

Figure 7. (a) Cyclic and (b) differential pulse voltammograms of **2b** in 0.1 M n-Bu_4NBF_4/THF solution at room temperature. $E_{1/2}(Cp_2Fe/Cp_2Fe^+) = +0.20$ V vs. Ag/Ag^+.

Table 3. Redox Potentials[a] (V vs. Ag/Ag^+) of Diphosphenes **1** and **2**, and Anthracene

Compound	E_{pc}	E_{pa}	$E_{1/2}$	Ref
1a	−1.84	−1.62	−1.73	16
	−2.42	−2.22	−2.32	
1b	−1.75	−1.57	−1.66	This work
	−2.33	−2.16	−2.25	
2a	−1.74	−1.47	−1.61[b]	This work
	−3.07	—	—	
2b	−1.81	−1.37	−1.59[b]	This work
	−3.07	−2.74	−2.91	
TbtP=PTbt	−2.00	−1.86	−1.93	16
Anthracene	−2.68	−2.16	−2.42	16

a) 0.1 M n-Bu_4NBF_4 in THF, $E_{1/2}(Cp_2Fe/Cp_2Fe^+) = +0.20$ V vs. Ag/Ag^+. b) Two-electron reduction.

affinity (EA) of the model compounds of DmpP=P(9-Anth) (**8**) and DmpP=PDmp (**9**) at B3LYP/6-311+G(2d) for P, 6-31G(d) for C, H level showed that the one-electron reduction of **8** should be more exothermic (1.27 eV) than that of **9** (1.06 eV), supporting the experimental results. Whereas the optimized structure of the anion radical species of **9** shows a geometry similar to that of the neutral species of **9** with the aryl rings of the Dmp group perpendicularly oriented to the P=P π-orbitals, the optimized geometry of the anion radical species of **8** exhibits considerable coplanarity between the π-electron planes of the anthryl and P=P moieties in contrast to the geometry of **8**, indicating the extension of π-electron conjugation in [$\mathbf{8}^{\bullet-}$].

Both bisdiphosphenes **2a** and **2b** showed one reversible two-electron reduction couple at $E_{1/2} = -1.61$ (**2a**) and -1.59 V (**2b**) versus Ag/Ag^+ together with further reduction waves (the pseudo-reversible reduction at $E_{pc} = -3.07$ V for **2a**, one-electron reduction couple at $E_{1/2} = -2.91$ V ($E_{pc} = -3.07$ V) for **2b**). The first reduction potentials of **2** ($E_{1/2} = -1.61$ V for **2a** and -1.59 V for **2b**) at a less negative region compared to those of monodiphosphene **1** ($E_{1/2} = -1.73$ V for **1a** and -1.66 V for **1b**) indicate that the connection of another P=P unit to anthryldiphosphene **1** leads to further stabilization of the anion species of **2** by the extended delocalization of the two P=P and the anthryl moieties in solution. The two-electron reductions of **2a** and **2b** should occur at once even under several conditions with the rate of scan from 20 to 200 mV s^{-1}, indicating little electronic communication between the two P=P moieties, in contrast to the case of diphosphenes **10** and **11** bearing ferrocenyl or p-phenylene unit as a linkage of two P=P moieties (Figure 8), which were reported to show the two-step one-electron reductions at two different potentials ($\Delta E_{1/2}$ = ca. 0.35 V).[11f,12h] Whereas the second reduction for **2b** ($E_{1/2} = -2.91$ V) was cleanly observed as reversible one-electron reduction, that for **2a** ($E_{pc} = -3.07$ V) was observed as pseudo-reversible reduction under the same conditions presumably due to the lower solubility of trianion species of **2a**.[27]

UV–Vis Spectra of Anthryldiphosphenes 1 and 2. Generally, the P=P chromophores of diphosphenes are known to show two characteristic absorption maxima, which are reasonably assigned to the symmetry-allowed π–π^*(P=P) electron transitions and symmetry-forbidden n–π^* electron

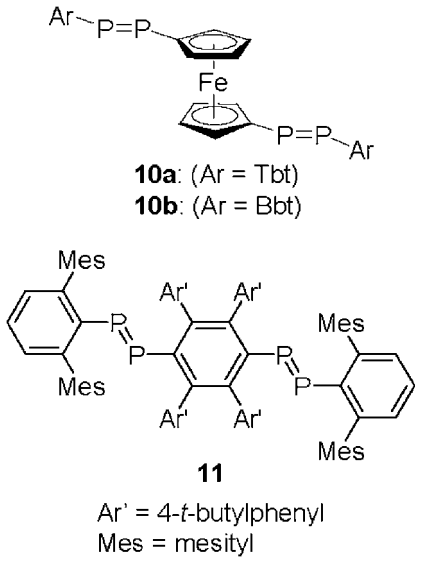

Figure 8.

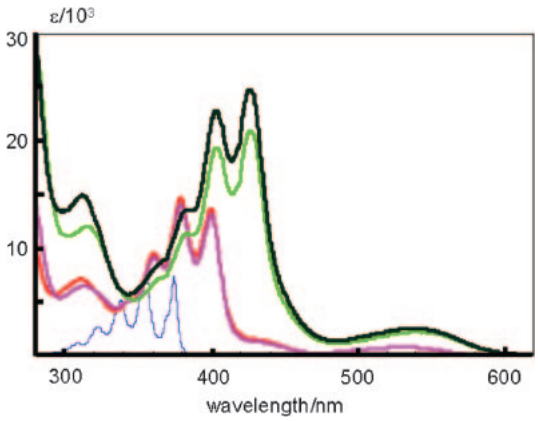

Figure 9. UV–vis spectra of **1a** (red), **1b** (pink), **2a** (dark green), **2b** (light green), and anthracene (dark blue) in hexane solution.

Table 4. UV–Vis Spectral Data of **1a**, **1b**, **2a**, and **2b** in Hexane Solution (λ_{max}/nm ($\varepsilon/10^3$))

1a	1b	2a	2b	Assignment[b)]
530 (0.78)	532 (0.79)	538 (2.5)	542 (2.2)	Anth $\pi \rightarrow$ P=P π^*
438 (sh, 1.3)	437 (sh, 1.2)	—[a)]	—[a)]	PP $n_- \rightarrow$ P=P π^*
400 (14)	400 (13)	426 (25)	427 (21)	Anth $\pi \rightarrow$ Anth π^*
380 (15)	380 (14)	403 (23)	404 (20)	Anth $\pi \rightarrow$ P=P π^*
361 (9.5)	361 (9.1)	382 (13)	383 (12)	
310 (7.2)	314 (6.5)	312 (14)	315 (12)	P=P $\pi \rightarrow$ P=P π^*

a) Not observed. b) Determined by the TDDFT calculations for **8** and **12** at TD-B3LYP/6-31+G(2d,p)//B3LYP/6-311+G(2d) for P and 6-31G(d) for C, H level.

transitions.[1a] However, the UV–vis spectra for **1a**, **1b**, **2a**, and **2b** in hexane solution showed complicated patterns due to several kinds of π–π^* electron transitions of the anthryl moiety together with those of the P=P moiety in the visible

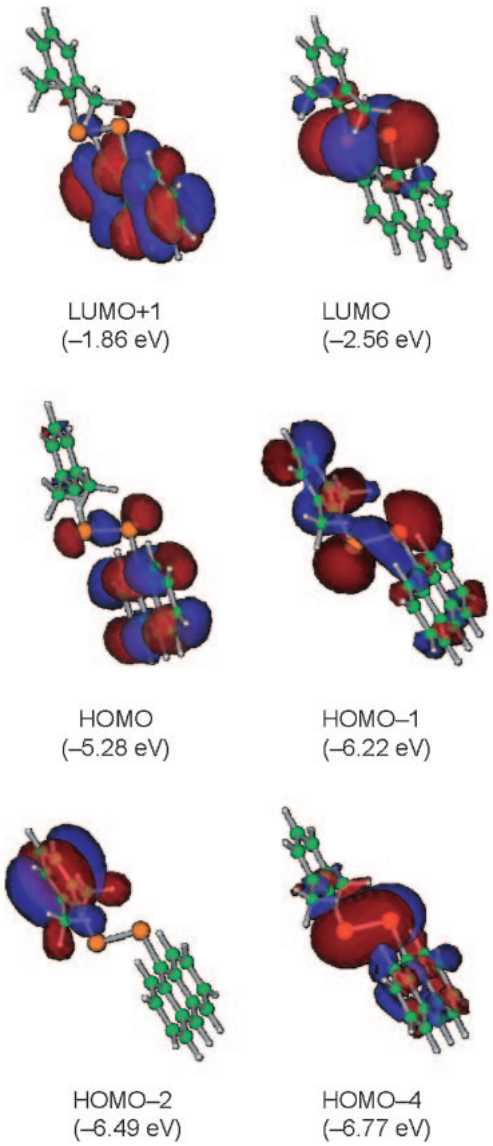

Figure 10. Selected molecular orbitals of DmpP=P(9-Anth) (**8**) (white; hydrogen, green; carbon, orange; phosphorus) calculated at B3LYP/6-31G(d) for C, H and 6-311+G(2d) for P level.

region. They are shown in Figure 9 together with that for the parent anthracene in hexane solution, and their λ_{max} values are shown in Table 4 together with their assignment on the basis of the TDDFT calculations of the model compounds of monodiphosphene, DmpP=P(9-Anth) (**8**), and bisdiphosphene, MeP=P($C_{14}H_8$)P=PMe (**12**, $C_{14}H_8$ = 9,10-anthrylene; both *syn*- and *anti*-configurations). Selected molecular orbitals of **8**, *syn*-**12**, and *anti*-**12** are shown in Figure 10, Figure S1, and Figure S2 (Supporting Information), respectively. Since the absorption patterns of **1a** and **1b** or **2a** and **2b** are similar to each other, the difference of the electronic perturbation of Tbt and Bbt should be negligible. The strong absorptions assignable to the π–π^*(Anth) transitions (HOMO–LUMO+1 transitions for monodiphosphene **8**) were observed in the range of 360–400 nm for **1** and 380–430 nm for **2**, and were in the longer wavelength region as compared with those of anthracene (335–

375 nm). The fact that the first and second introduction of a diphosphene (P=P) unit toward the central anthracene moiety causes apparent red-shift by ca. 25 nm as compared with that of anthracene and monodiphosphene derivative, respectively, may imply somewhat extended π-electron conjugation in solution. The ε values of the π–π^*(Anth) transitions also increased by the introduction of the diphosphene (P=P) unit toward the central anthracene moiety. In the longer wavelength region compared with those of the π–π^*(Anth) transitions, two weak absorptions were observed. One of the absorptions assignable to the n–π^*(P=P) transitions, which are known to be observed in the cases of many stable diphosphenes, was observed at 438 nm for **1a** and at 437 nm for **1b** as shoulders (HOMO−1–LUMO transition), respectively, whereas those for bisdiphosphenes **2** were not observed probably due to the strong absorptions of the symmetry-allowed π–π^*(Anth) transitions. The other one was observed as an absorption at the longest wavelengths (530 nm for **1a**, 532 nm for **1b**, 538 nm for **2a**, and 542 nm for **2b**). The λ_{max} of bisdiphosphenes **2** were red-shifted by ca. 10 nm and the ε values were about three times larger than those of the corresponding monodiphosphene **1**. It is worthy of note that these transitions are attributable to π(9-Anth)–π^*(P=P) transition (HOMO–LUMO transition for monodiphosphene **8**), strongly indicating the electronic correlation between the anthryl and P=P moieties.[28] The HOMO of **8** dominantly exhibits the π-character of anthracene associated with the small contribution of P–P (σ) bond and the lone-pair, while the LUMO exhibits the low-lying π^* character of the P=P unit. On the other hand, the π–π^*(P=P) transitions (HOMO−4–LUMO transition for monodiphosphene **8**), which are known to be observed as a strong absorption in the cases of many stable diphosphenes, observed at 310 (**1a**), 314 (**1b**), 312 (**2a**), and 315 nm (**2b**) were relatively shorter values as compared with those of the previously reported diaryldiphosphenes.[1a,4f] The differences of the observed absorption maxima for the π–π^*(P=P) transitions between monodiphosphenes **1a** and **1b** and bisdiphosphenes **2a** and **2b** are only 2 and 1 nm, respectively, indicating the less effective π-electron conjugation between the anthryl and P=P moieties in solution. The ε values of bisdiphosphenes **2** were approximately twice as large as those of monodiphosphenes **1**. Therefore, the red shifts of π–π^*(Anth) transitions mentioned above should be explained by the σ-conjugation effect of the P–C bonds. For example, similar tendency was observed in their precursors, dichlorophosphinoanthracenes **4** and **5**, which showed their π–π^*(Anth) transitions around 345–405 and 365–435 nm, respectively, in the longer wavelength region as compared with those of anthracene.[29]

Photophysical Behavior of 9-Anthryldiphosphene 1a. 9-Anthryldiphosphene **1a** in hexane solution displayed very weak, but apparent, light-blue emission. To the best of our knowledge, this is the first fluorescence spectral data of a diphosphene. The fluorescence spectrum showed a broad wave pattern in the range of ca. 400–500 nm ($\lambda_{max} = 432$ nm) by using the excitation wavelength at 400 nm, while no emission was observed by the excitation at 530 nm, which was the longest λ_{max} of **1a** (Figure 11a). Accordingly, the observed emission should be due to S_n–S_0 ($n \neq 1$) transitions, since the HOMO–LUMO and HOMO−1–LUMO transitions should be symmetry-forbidden. The fact that the excitation spectra by using the emission wavelength at 432 nm were similar to the UV–vis spectra of **1a** strongly suggests the emission was generated from not the other highly emissive impurities but the anthryldiphosphene **1a**. The quantum yield of **1a** was 1.2×10^{-3}, which is 0.44% compared to that of anthracene observed under the same conditions.[30] The weakness of the fluorescence of **1a** might be due to the quenching by the lone pair of the phosphorus atom[31] or the deformation of the structure in the excited state. On the other hand, the emission intensity at low temperature (at −95 °C) increased ca. 1.3 fold over that at room temperature (Figure 11b). The observed lifetime of the photoluminescence of **1a** was 7–10 ns, which is slightly longer than that of anthracene (5.75 ns),[32] indicating the luminescence of **1a** should be not phosphorescence but

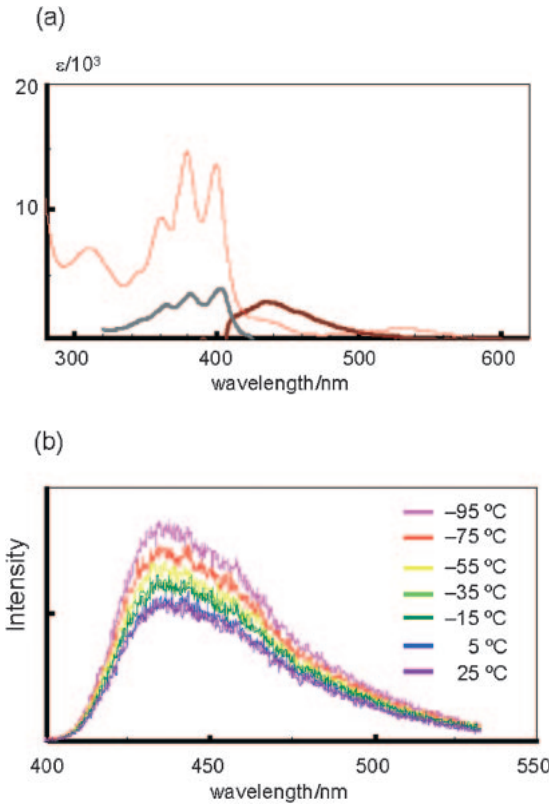

Figure 11. (a) UV–vis (red), excitation (em. 432 nm; gray), and fluorescence (ex. 400 nm; brown) spectra of **1a** in hexane solution. (b) Variable temperature fluorescence (ex. 400 nm) spectra of **1a** in hexane solution.

Table 5. Lifetime of the Photoluminescence (ns) of **1a**

T/°C	Wavelength/nm		
	406–438	438–473	473–533
−95	7.7 ± 0.6	7.5 ± 0.6	9.4 ± 0.9
−75	7.8 ± 0.8	7.4 ± 0.8	9.0 ± 1.7
−55	7.9 ± 0.9	7.9 ± 0.5	9.3 ± 1.4
−35	7.6 ± 1.0	6.6 ± 0.8	9.1 ± 1.2
−15	7.0 ± 0.9	7.2 ± 0.8	9.5 ± 1.1
5	7.4 ± 0.8	7.0 ± 0.6	9.3 ± 1.5
25	6.8 ± 0.8	6.9 ± 0.8	8.9 ± 1.1

fluorescence (Table 5). The lifetime measurement in the range up to 20 μs showed no other emission indicative of phosphorescence. For the analysis of lifetime of the fluorescence of **1a**, the time-resolved emission spectra were measured separately in the three regions of wavelength (406–438, 438–473, and 473–533 nm) as shown in Table 5, and each lifetime for the whole wavelength region of the three was obtained. As a result, fluorescence in a longer wavelength region (473–533 nm) has somewhat longer lifetime than that at shorter wavelengths (406–473 nm) by ca. 2 ns. The reason is unclear at present. In contrast to anthryldiphosphene **1a**, however, TbtH, TbtP=PTbt, and bisdiphosphenes **2a** and **2b** exhibited no appreciable luminescence under the same conditions.

Complexation of 9-Anthryldiphosphene 1a. As shown above, the connection of a diphosphene unit to the anthryl moiety brought about decrease in photoluminescence of the anthracene moiety probably due to quenching by the phosphorus lone pair. On the other hand, anthrylphosphine oxides[31,33] and gold complexes[34] of anthrylphosphine derivatives are reported to exhibit intense fluorescence, giving suggestive information that the capping of the lone pair on phosphorus has possibility to increase the intensity of the photoluminescence. The diphosphene oxide, [Mes*P=P(=O)Mes*],[35] and the cationic diphosphene gold complex, {[Mes*P=P(AuPEt$_3$)-Mes*]PF$_6$},[36] are reported but not isolated as a stable compound. Very recently, Protasiewicz and his co-workers have succeeded in the isolation of the gold complexes of diphosphene, Mes*{AuCl}P=PMes* and Mes*{AuCl}P=P{AuCl}Mes*, as a stable solid.[37]

Diphosphenes are known to coordinate various transition metals in the η^1 (end-on) and/or η^2 (side-on) fashions with the lone-pair electrons of phosphorus atoms or the π-orbitals of diphosphene (P=P) moiety, respectively.[1a,38] In the case of the carbonyl complexes of transition metals, such as chromium, iron, and nickel, the diphosphenes were found to coordinate toward the metal center in the η^1 fashion. Especially, Yoshifuji and his co-workers reported that the reaction of the diphosphene, Mes*P=PMes, with [Cr(CO)$_5$(thf)] gave the corresponding chromium complex, (*E*)-Mes*P=P{Cr(CO)$_5$}Mes, where the phosphorus atom bearing a less hindered substituent, i.e., mesityl group, selectively coordinated to the chromium center.[39] Therefore, the complexation of **1a** toward the chromium metal was examined in the expectation of obtaining diphosphene complex with relatively intense photoluminescence as compared with **1a**.

Treatment of **1a** with excess amount of [Cr(CO)$_5$(thf)] in the dark resulted in the exclusive formation of the expected η^1-chromium complex, (*E*)-TbtP=P{Cr(CO)$_5$}(9-Anth) (**13**) (Scheme 3). The ^{31}P NMR spectra showed characteristic AB quartet signals at δ 422.6 and 519.8 with the coupling constant of $^1J_{PP}$ = 527 Hz, the data of which were similar to those of (*E*)-Mes*P=P{Cr(CO)$_5$}Mes (δ_P 412.3, 500.9 and $^1J_{PP}$ = 517.6 Hz).[39] Thus, the P=P double-bond character should remain in the chromium complex **13**. Chromium complex **13** was stable toward air and moisture but somewhat unstable toward light.

In Figure 12 was shown the structure of chromium complex **13**, which was established by the X-ray crystallographic analysis of single crystals obtained by the recrystallization from its toluene solution. The phosphorus atom bearing the less hindered anthryl unit was found to coordinate to the chromium center in an η^1 fashion and the aryl groups of the diphosphene unit were located in the (*E*)-configuration. The coplanarity of the four atoms, Cr, P1, P2, and C1, was supported by the sum of the bond angles around the P1 atom at 360.0°. The phosphorus–phosphorus bond length of the chromium complex **13** [2.0307(10) Å] is similar to that of diphosphene **1a** [2.0352(16) Å], indicating its P=P double-bond character (Table 1). The P1–Cr bond distance 2.3104(8) Å is somewhat shorter than those of the previously reported (*E*)-diphosphene–chromium complexes [2.33–2.41 Å].[40]

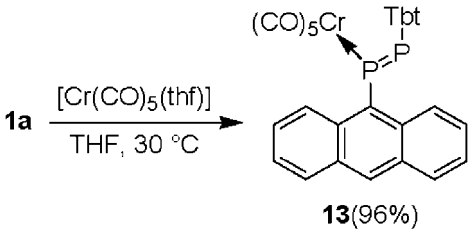

Scheme 3. Reaction of **1a** with [Cr(CO)$_5$(thf)].

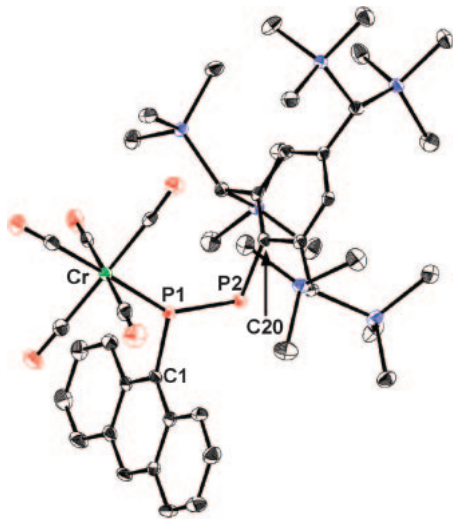

Figure 12. Molecular structure of chromium complex **13** with thermal ellipsoid plot (50% probability). Hydrogen atoms are omitted for clarity. Selected bond length (Å) and angles (°): P(1)–Cr 2.3104(8), C(1)–P(1)–Cr 116.32(9), P(2)–P(1)–Cr 141.59(4).

The complexation of anthryldiphosphene to Cr(CO)$_5$ moiety brought about a drastic change in the UV–vis absorption. In Figure 13 is shown the UV–vis spectra of **13** together with that of anthryldiphosphene **1a**. An intense and broad absorption was observed in the range of 420–550 nm with the absorption maximum at 465 nm, which is similar to that of Mes*P=P{Cr(CO)$_5$}Mes (λ_{max} = 460 nm).[39] This transition is most likely attributable to the metal to ligand charge transfer (MLCT) transitions in consideration of the low-lying LUMO level of a diphosphene.[41] Despite the introduction of the Cr(CO)$_5$ moiety onto the diphosphene unit, the π–π^* electron transitions of the anthryl moiety of **13** (360, 378, and 400 nm) are nearly the same as those of **1a**, indicating almost no electronic perturbation from the chromium moiety.

Chromium complex **13** exhibited no appreciable luminescence by using the excitation wavelength at 400 and 465 nm. The gold complexes of diphosphene, Mes*{AuCl}P=PMes* and Mes*{AuCl}P=P{AuCl}Mes*, were reported to show no fluorescence.[37] Although the reason for no apparent photoluminescence of the diphosphene complexes is unclear at present, the complexation of diphosphene toward the metal center might not be effective for the improvement of the photoluminescence ability of a diphosphene.

Chalcogenation of Anthryldiphosphene 1b. Next, we examined the reactions of the newly obtained diphosphene **1b** with chalcogenation reagents such as elemental sulfur, selenium, and tributylphosphine telluride, in the expectation of obtaining unique heterocyclic compounds composed of several numbers of heteroatoms.[42–45] The reaction conditions of the chalcogenation reactions of **1b** were summarized in Scheme 4.

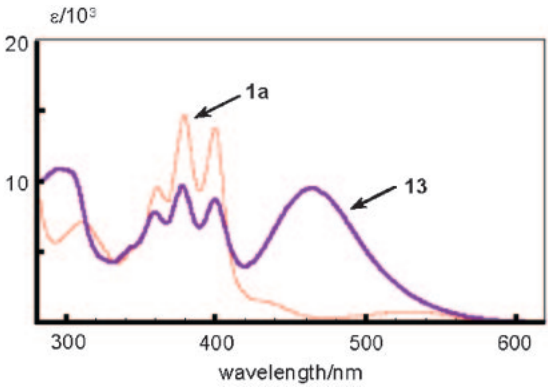

Figure 13. UV–vis spectra of **1a** (red) and **13** (purple) in hexane solution.

The reaction of **1b** with 1.2 equiv of elemental sulfur at room temperature and 5 equiv of elemental selenium at 80 °C in C_6D_6 afforded the corresponding three-membered ring compounds, thia- and selenadiphosphiranes **14** and **15** as yellow crystals in 69 and 84% isolated yields, respectively. The ^{31}P NMR spectra of **14** and **15** showed AB quartet signals at δ −81.9, −80.3 ($^1J_{PP}$ = 227 Hz) for **14** and δ −70.2, −63.5 ($^1J_{PP}$ = 240 Hz) together with satellite signals with $^1J_{PSe}$ = 125, 123 Hz for **15**, respectively. The observed ^{31}P chemical shifts and coupling constants, $^1J_{PP}$ and $^1J_{PSe}$, were similar to those of the previously reported diarylsubstituted thia- and selenadiphosphiranes (δ_P −84.0– −47.4, $^1J_{PP}$ = 233–247 Hz, $^1J_{PSe}$ = 121–132 Hz).[4f,42–44] In the case of sulfurization reaction of **1b**, unidentified products **16a** and **16b** other than **14** was observed in the crude mixture. The ^{31}P NMR spectra of **16a** and **16b** were δ 197.5, 279.2 ($^1J_{PP}$ = 600 Hz) and δ 222.3, 237.4 ($^1J_{PP}$ = 615 Hz), respectively. On the basis of the chemical shifts and the coupling constant of diphosphene monosulfide, Mes*P=P(=S)Mes*, reported by Yoshifuji et al. (δ 255.8, 247.8, $^1J_{PP}$ = 633.9 Hz),[42a,42b] unidentified products **16a** and **16b** are attributable to the two different types of diphosphene monosulfides, Bbt(S=)P=P(9-Anth) and BbtP=P(=S)(9-Anth). It should be noted that the signal of **15** in the ^{77}Se NMR spectra was observed considerably downfield at δ 72.0 as a pseudotriplet ($^1J_{SeP}$ = 123 Hz), compared to that of BbtP(Se)PBbt (**17**, δ 14.6).[4f] To get information on the difference of the chemical shifts of the selenadiphosphiranes, theoretical calculations of model compounds, MesP(Se)P(9-Anth) (**18**) and MesP(Se)PMes (**19**), bearing mesityl (Mes) groups instead of Bbt groups were carried out at GIAO-B3LYP/6-311+G(2d,p)//B3LYP/6-31G(d) (TZ(2d) for P, Se) level. The P–P and P–Se bond lengths of the optimized

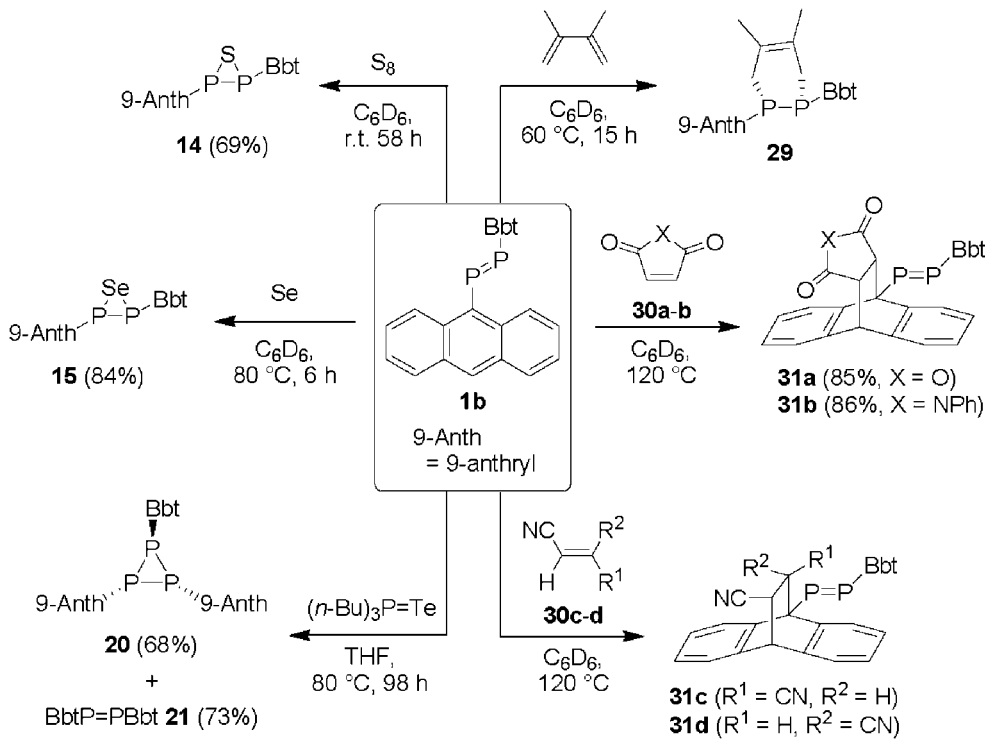

Scheme 4. Reactivities of **1b**.

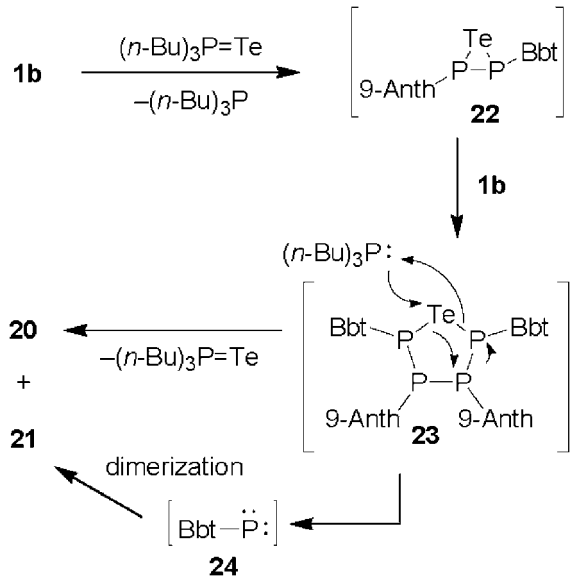

Scheme 5. Postulated mechanism for the formation of **20**.

structures of **18** and **19** were slightly longer than those of the experimentally observed structures (vide infra). Selected bond lengths and angles are shown in Table 6. The ^{77}Se NMR chemical shifts for **18** and **19** were computed to be δ 151 and −138, respectively, supporting the low-field shifted values of **15** as compared with that of BbtP(Se)PBbt. Although the reason why it was observed in the downfield region compared with that of other selenadiphosphiranes was unclear, the anthryl moiety of **1b** may afford some electronic effect toward the selenium atom.

The successful sulfurization and selenization reactions of anthryldiphosphene **1b** have prompted us to examine the tellurization reaction in the expectation of obtaining telluradiphosphirane.[44,45] The reaction of **1b** with excess amount of $(n\text{-Bu})_3$P=Te[46] at 80 °C for 98 h in a sealed tube gave triphosphirane **20** and BbtP=PBbt (**21**) in 68 and 73% yields, respectively, without formation of the corresponding telluradiphosphirane derivative. Since $(n\text{-Bu})_3$P=Te was almost quantitatively recovered in this reaction, and heating of 9-anthryldiphosphene **1b** in the absence of $(n\text{-Bu})_3$P=Te under the same conditions (in THF at 80 °C for 98 h) resulted in the almost quantitative recovery of **1b** along with the formation of a trace amount of triphosphirane **20** and an unidentified mixture, $(n\text{-Bu})_3$P=Te should work as a catalyst in the thermal reaction of **1b** leading to the formation of **20** and **21** under these conditions. In the ^{31}P NMR spectrum, triphosphirane **20** showed characteristic A_2B-pattern signals in the high-field region at δ −92.9 (doublet) and δ −127.4 (triplet) with the coupling constant of $^1J_{PP}$ = 188 Hz. Since the observed NMR spectral data (δ_P and $^1J_{PP}$ value) of **20** are similar to those of the previously reported triphosphiranes,[47] the bulky substituents, Bbt and 9-anthryl groups, might not be electronically and sterically so effective toward the central triphosphirane skeleton. The X-ray crystallographic analyses also supported the structure of **20**.[48]

The postulated mechanism for the formation of **20** is shown in Scheme 5. First of all, telluradiphosphirane **22** may be generated by the reaction of anthryldiphosphene **1b** with $(n\text{-Bu})_3$P=Te as in the case of sulfurization and selenization reactions of **1b**. Telluradiphosphirane **22** thus generated, which would be highly reactive due to the high strain of the three-membered ring system, undergoes an insertion reaction of the remaining **1b** into the P–Te bond giving telluratetraphospholane **23**, where the P atom adjacent to the Te atom would have a Bbt group. The stereoselective insertion reaction would occur due to the severe steric hindrance of the Bbt group. Then, $(n\text{-Bu})_3$P generated by the initial reaction of anthryldiphosphene **1b** with $(n\text{-Bu})_3$P=Te would attack the tellurium atom of **23** to afford the corresponding triphosphirane **20** and phosphinidene **24**, which should undergo ready dimerization leading to the formation of BbtP=PBbt (**21**).

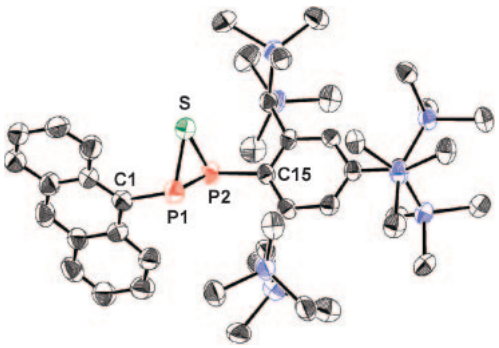

Figure 14. Molecular structure of **14** with thermal ellipsoid plot (50% probability). Hydrogen atoms are omitted for clarity.

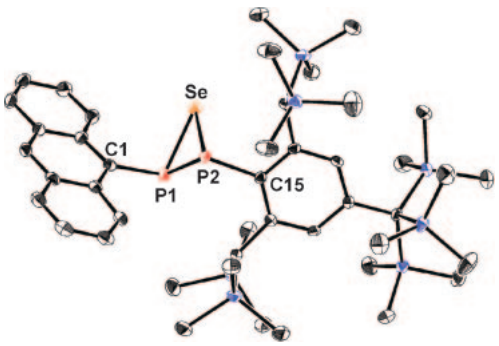

Figure 15. Molecular structure of **15** with thermal ellipsoid plot (50% probability). Hydrogen atoms are omitted for clarity.

The X-ray crystallographic analysis revealed the structural parameters of chalcogenadiphosphiranes **14** and **15** as shown in Figures 14 and 15. Selected bond lengths and angles are given in Table 6 together with those of related compounds.[4f,42d,43b,43c] In thia- and selenadiphosphiranes, **14** and **15**, the two substituents (9-Anth and Bbt) are located in an *E* configuration with respect to the central chalcogenadiphosphirane skeleton. The P–P bond lengths of **14** [2.230(2) Å] and **15** [2.2172(9) Å] are considerably longer than that of anthryldiphosphene **1b** [2.0232(13) Å]. The P–E (E = S or Se) bond lengths of **14** and **15** are 2.121(2) and 2.158(2) Å for **14** and 2.2655(6) and 2.2825(7) Å for **15**, respectively. These values are similar to typical P–P single bond lengths (ca. 2.2 Å)[49] and the sum of the covalent radii of P and E atoms (2.14 Å for P–S and 2.27 Å for P–Se single bonds, respectively).[50] The P–E

Table 6. Observed and Calculated Structural Parameters for **14**, **15**, **18**, and **19** together with Related Compounds

Compound	Bond lengths/Å			Bond angles/°			Ref.
	P1–P2	P1–E	P2–E	E–P1–P2	E–P2–P1	P1–E–P2	
E = S							
14[a)]	2.230(2)	2.121(2)	2.158(2)	59.40(8)	57.79(7)	62.81(8)	This work
25[a)]	2.2349(12)	2.1083(18)	2.1285(12)	58.61(4)	57.72(4)	63.67(4)	4f
26[a)]	2.249(3)	2.103(3)	2.103(3)	57.7(1)	57.7(1)	64.6(1)	42d
E = Se							
15[a)]	2.2172(9)	2.2655(6)	2.2825(7)	61.21(2)	60.44(2)	58.35(2)	This work
17[a)]	2.250(3)	2.250(3)	2.270(3)	60.59(9)	59.71(9)	59.70(8)	4f
27[a)]	2.202(3)	2.268(2)	2.266(3)	60.9(1)	61.0(1)	58.1(1)	43c
28[a)]	2.231(1)	2.257(1)	2.253(1)	60.26(3)	60.44(3)	59.30(3)	43b
18[b)]	2.271	2.318	2.319	60.71	60.64	58.65	This work
19[b)]	2.257	2.315	2.337	61.48	60.47	58.05	This work

a) Observed values. b) Calculated values at B3LYP/6-31G(d) for C, H and TZ(2d) for P, Se level.

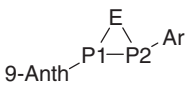

14 (E = S, Ar = Bbt)
15 (E = Se, Ar = Bbt)
18 (E = Se, Ar = Mes)

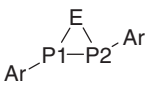

17 (E = Se, Ar = Bbt)
19 (E = Se, Ar = Mes)
25 (E = S, Ar = Bbt)
26 (E = S, Ar = Mes*)
27 (E = Se, Ar = Cp*)
28 (E = Se, Ar = $C_6H_2(CF_3)_3$)

bonds bearing a Bbt group on the phosphorus atom are somewhat longer than those bearing a 9-anthryl group. Therefore, it was found that thia- and selenadiphosphiranes **14** and **15** have a three-membered ring with single bonds, and exhibit almost no π-complex character, which is often seen in charcogenadisiliranes.[4f]

Cycloaddition Reaction of Anthryldiphosphene 1b with a Diene and Electron-Deficient Olefins. Treatment of **1b** with excess 2,3-dimethyl-1,3-butadiene in C_6D_6 at 60 °C in a sealed NMR tube afforded the corresponding [4 + 2] cycloadduct **29** in 67% isolated yield (Scheme 4). Thus, the high reactivity of the central P=P unit of **1b** toward Diels–Alder reaction was demonstrated by the [4 + 2] cycloaddition reaction of **1b** with 2,3-dimethyl-1,3-butadiene, even though it is well sterically protected by the Bbt group. The ^{31}P NMR spectra of **29** showed AB quartet signals at δ −58.2, −57.4 with coupling constant of $^1J_{PP} = 208$ Hz, similarly to the previously reported diene adduct (1-*t*-butyl-2-mesityl-4,5-dimethyl-1,2-diphosphacyclohex-4-ene; δ −58.8, −12.5, $^1J_{PP} = 229$ Hz).[51] Other spectroscopic data and the X-ray crystallographic analysis (Figure 16) also supported the structure of **29**.

All the reactions of anthryldiphosphene **1** described above are derived from the highly reactive P=P unit as is the case of the previously reported diphosphene derivatives. In fact, only a few examples have been reported for substitution reactions on the phosphorus atom.[52] To the best of our knowledge, there has been no example of transformation reactions by the functionalization of the substituent on the P=P moiety while keeping the reactive P=P unit intact. Since anthryldiphosphene **1** possesses another reactive site, the anthryl unit, in its molecular skeleton together with the highly reactive P=P unit, we have focused on the reactivity of the anthryl unit of anthryldiphosphene **1**. The HOMO of the model compound DmpP=P-(9-Anth) (**8**), which has significant π-character of the anthryl moiety, indicates that the anthryl moiety of **1** can be the

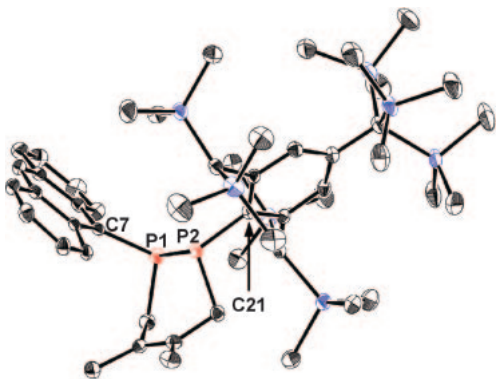

Figure 16. Molecular structure of **29** with thermal ellipsoid plot (50% probability). Hydrogen atoms are omitted for clarity.

reactive site. Since anthracene derivatives are known to undergo Diels–Alder cycloaddition with various electron-deficient olefins,[53] we examined the reaction of **1b** with electron-deficient olefins.[19,54]

The reaction of **1b** with 3 equiv of maleic anhydride (**30a**) and *N*-phenylmaleimide (**30b**) in C_6D_6 at 120 °C in a sealed NMR tube resulted in the exclusive formation of the corresponding [4 + 2] cycloadducts **31a** and **31b** in 85 and 86% isolated yields, respectively (Scheme 4). Likewise, the reactions of **1b** with an excess amount (30 equiv) of fumaronitrile (**30c**) and maleonitrile (**30d**) resulted in the exclusive formation of **31c** and **31d** in 83 and 71% isolated yields, respectively. The transformation of **1b** into alkylaryldiphosphene derivatives **31** via the Diels–Alder reactions should be of great note as a unique example of the transformation of a diphosphene into other diphosphenes while keeping the highly reactive diphosphene unit.

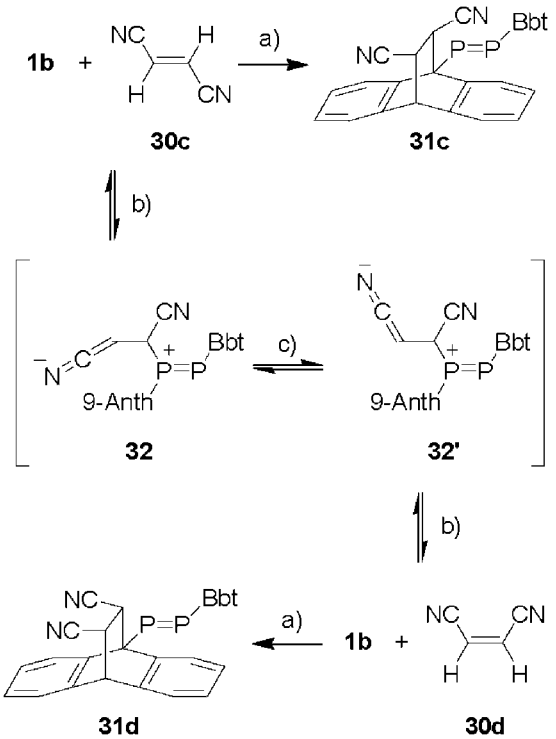

Scheme 6. Plausible mechanism for the isomerization of fumaronitrile (**30c**) into maleonitrile (**30d**). a) [4 + 2] cycloaddition, b) addition/elimination, and c) rotation.

On the other hand, treatment of **1b** with 5 equiv of fumaronitrile (**30c**) in C_6D_6 at 120 °C for 72 h afforded the two types of [4 + 2] cycloadducts, **31c** (44% isolated yield) and **31d** (15% isolated yield), together with the starting material **1b** and maleonitrile (**30d**). Since it is interesting that **31c** and **31d** were obtained in the reaction of **1b** with **30c**, we have investigated the reaction mechanism as follows. The fact that the isolated cycloadducts **31c** and **31d** did not isomerize toward each other under the same conditions used for the reaction of **1b** with **31c** strongly implies the isomerization of fumaronitrile leading to the formation of maleonitrile during the reaction. The isomerization of **30c** is most likely interpreted in terms of the zwitterionic intermediate **32**, which might be generated by the reaction of **1b** with **30c** as shown in Scheme 6.[55] The phosphorus atom of **1b** bearing the anthryl group may attack the C=C bond of **30c** due to steric reasons to give **32**, which may retain its P=P double-bond analogously to a previous report of an isolated phosphanyl phosphenium ion, $[Mes^*P{=}P(Me)Mes^*]^+$ bearing significant P=P double-bond character.[56] Taking into consideration the zwitterionic species **32**, the π-bond of the (NC)C=C(CN) moiety of **32** should be weakened enough to be rotated along with the C–C axis to give **32′**. Then, the cleavage of the P–C bond of **32′** should occur to afford **1b** and maleonitrile. Maleonitrile thus generated should react with **1b** to give the maleonitrile adduct **31d** as in the case of the reaction of **1b** with fumaronitrile leading to the formation of **31c**. In fact, the isomerization of **30c** into **30d** was observed by ^{1}H NMR spectra when **30c** was treated with a small amount of BbtP=PBbt in C_6D_6 at 120 °C, whereas no change was observed on heating of a C_6D_6 solution of **30c** at 120 °C for 60 h. In addition, the reaction of **30c** in the presence of 20 mol % of anthracene under the same reaction conditions used for **1b** and **30c** only gave the corresponding [4 + 2] cycloadduct of fumaronitrile and the unreacted **30c**. Neither [4 + 2] cycloadduct of maleonitrile nor maleonitrile (**30d**) was observed in the ^{1}H NMR spectra after additional heating for 48 h. These results strongly suggested that not the anthryl unit but the phosphorus atoms of the P=P unit should take part in the isomerization of **30c**.

The newly obtained diphosphenes **31a**, **31c**, and **31d** were found to undergo retro-Diels–Alder reaction on heating at 120 °C, whereas maleimide adduct **31b** did not dissociate into **1b** and maleimide **30b** even on heating at 120 °C for 48 h. Heating C_6D_6 solutions of diphosphenes **31a**, **31c**, and **31d** in the presence of 10 equiv of **30b** as a trapping reagent of anthryldiphosphene **1b** in a sealed NMR tube at 120 °C for 24 h gave the starting diphosphenes **31**, the maleimide adduct **31b** generated via the [4 + 2] cycloaddition of **1b** with **30b**, and the corresponding olefins **30** in the ratio of 88/12/4 (**31a**/**31b**/**30a**) for **31a**, 83/17/4 (**31c**/**31b**/**30c**) for **31c**, and 63/37/18 (**31d**/**31b**/**30d**) for **31d**, respectively, judging from the signal of the ^{1}H NMR spectra. Thus, the retro-Diels–Alder reactions of **31a**, **31c**, and **31d** were found to proceed as fast in the order of **31d** > **31c** > **31a**.

The ^{31}P NMR spectra of **31a**–**31d** showed characteristic AB quartet signals (**31a**: δ 520.3, 571.2, $^1J_{PP} = 583$ Hz; **31b**: δ 525.8, 564.3, $^1J_{PP} = 577$ Hz; **31c**: δ 518.8, 579.4, $^1J_{PP} = 592$ Hz; **31d**: δ 522.6, 578.3, $^1J_{PP} = 592$ Hz) in the low field region, respectively, supporting their P=P double-bond character similar to those observed for **1**. Moreover, as a result of the [4 + 2] cycloaddition of **1b** with **30a**–**30d**, the signal for the protons at the 10-position of the anthryl unit of **1b** was drastically shifted from 8.18 (**1b**) to 3.92–4.79 (**31**), due to the dearomatization of the central ring of the anthryl unit. The X-ray crystallographic analysis of **31a**–**31d** revealed the molecular structures of the newly obtained diphosphenes. The selected bond lengths and angles are tabulated in Table 1. The P=P bond lengths and P–P–C angles of [4 + 2] cycloadducts **31** are in the range of 2.022(2)–2.0383(18) Å and 100.34(12)–105.43(19)°, respectively, which are similar to those of anthryldiphosphenes **1** [2.0232(13)–2.0352(16) Å and 97.66(11)–105.81(11)°]. It should be worthy of note that the P1–C1 bond lengths of **1** and **31** are largely different from each other [1.838(4)–1.842(3) Å for **1** and 1.889(6)–1.903(4) Å for **31**, respectively] due to the change of the hybridization of C1 carbon atom from sp^2 (**1**) to sp^3 (**31**) along with the elongation of the P1–C1 bond lengths by ca. 0.05 Å.

The UV–vis spectra of **31a**–**31d** in hexane solution are shown in Figure 17, and the λ_{max} values are given in Table 7. The strong absorbance of **1b** observed around 360–400 nm attributable to the π–π^*(Anth) transitions vanished with the loss of the anthryl moiety by the [4 + 2] cycloaddition reaction. Absorption patterns of **31** are similar to each other and the three characteristic absorption maxima were observed around 490, 370, and 320 nm. The longest absorptions observed around 484–491 nm are assignable to the n–π^*(P=P) transitions on the basis of the TDDFT calculations of **33a**, which is a model compound of **31a** with a Dmp group instead of a Bbt group.[57] The second absorptions around 366–370 nm should be assign-

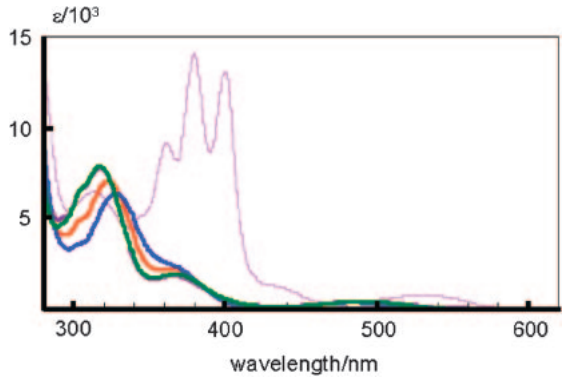

Figure 17. UV–vis spectra of **31a** (orange), **31b** (blue), **31c** (green), **31d** (purple), and **1b** (pink) in hexane solution.

Table 7. UV–Vis Spectral Data of **31a–31d** in Hexane Solution (λ_{max}/nm ($\varepsilon/10^3$))

31a	**31b**	**31c**	**31d**
487 (0.42)	484 (0.39)	490 (0.45)	491 (0.45)
370 (sh, 2.1)	369 (sh, 2.3)	369 (1.9)	366 (1.8)
323 (6.9)	328 (6.4)	317 (7.7)	317 (7.7)

able to π(Ph)–π^*(P=P) electron transitions. The third ones, which have large molar extinction coefficient, should be assignable to π–π^*(P=P) transitions along with the some contribution of π(Ph)–π^*(P=P) transitions. The λ_{max} values (317–328 nm) and molar extinction coefficient for **31** are similar to that of **1b**.

Conclusion

The first stable anthryldiphosphenes **1** and **2** were synthesized and characterized by spectroscopic and X-ray crystallographic analyses. The P=P bond character of **1** and **2** was supported by the NMR, Raman, IR spectroscopic data and X-ray crystallographic analyses. Cyclic voltammograms of **1** and **2** showed two reversible one-electron reduction couples for **1** and one reversible two-electron reduction couple together with the one electron reduction for **2**. The UV–vis spectra of **1** and **2** revealed the electronic communication between the anthryl and P=P units, which was supported by the TDDFT calculations. Monodiphosphene **1a** showed weak fluorescence in hexane solution, whereas bisdiphosphenes **2** exhibited no appreciable luminescence under the same conditions. Furthermore, the reaction of anthryldiphosphene **1** with a chromium complex, chalcogenation reagents, a diene, and electron-deficient olefins were examined, showing the unique reactivity of **1**. These results of the fundamental studies of anthryldiphosphene derivatives should be important for the molecular design of novel materials utilizing the characteristic properties of a P=P π-bond.

Experimental

All experiments were performed under an argon atmosphere unless otherwise noted. Solvents used for the reactions were purified by an Ultimate Solvent System (Glass Contour Co.).[58] All solvents used in the spectroscopy (benzene-d_6, cyclohexane-d_{12}, and hexane) were dried by using a potassium mirror. The ^{1}H NMR (400 or 300 MHz) and ^{13}C NMR (100 or 75 MHz) spectra were measured in C_6D_6, C_6D_{12}, or $CDCl_3$ with a JEOL JNM AL-400 or AL-300 spectrometer. Signals due to C_6D_5H (7.15 ppm), $C_6D_{11}H$ (1.38 ppm), and $CHCl_3$ (7.25 ppm) in ^{1}H NMR spectra and those due to C_6D_6 (128 ppm), C_6D_{12} (26.4 ppm), and $CDCl_3$ (77.0 ppm) in ^{13}C NMR spectra were used as internal references, respectively. ^{31}P NMR (121 MHz) spectra were measured in C_6D_6 or $CDCl_3$ with a JEOL AL-300 spectrometer using 85% H_3PO_4 in water (0 ppm) as an external standard. ^{77}Se NMR (75 MHz) spectra were measured in C_6D_6 with a JEOL AL-400 spectrometer using Ph_2Se_2 (460 ppm) as an external standard. Multiplicity of signals in ^{13}C NMR spectra was determined by DEPT, HMQC, CH-cosy, HMBC, and long-range CH-COSY techniques. High-resolution EI- and FAB-mass spectral data were obtained on a JEOL JMS-700 spectrometer. Raman spectra were measured on a Raman spectrometer consisting of a Spex 1877 Triplemate and an EG&G PARC 1421 intensified photodiode array detector. An NEC GLG 108 He–Ne laser was used for Raman excitation. Infrared spectra were recorded as KBr pellets using a JASCO FT/IR-460 Plus spectrometer. UV–vis spectra were measured on a JASCO Ubest V-570 UV–vis spectrometer in a glovebox filled with argon at ambient temperature or with a degassed quartz cell connected with a Pyrex® tube after freeze–pump–thaw at low temperature, respectively. Fluorescent spectra were measured using a JASCO Ubest FP-6600 with a quartz cell connected with a Young valve in which hexane solutions of each compounds were put filled with argon at ambient temperature. The quantum yields were determined comparing to a solution of anthracene in ethanol ($\Phi = 0.27$) as a reference.[30] Time-resolved fluorescent spectra were measured on a streak camera (Hamamatsu photonics, C5094) with regenerative amplifier Ti:Al_2O_3 laser (Spectra physics, Spitfire and optical parametric amplifier (OPA-800)). The electrochemical experiments were carried out with an ALS 602A electrochemical analyzer using a glassy carbon disk working electrode, a Pt wire counter electrode, and Ag/0.01 M $AgNO_3$ reference electrode. The measurements were carried out in THF solution containing 0.1 M n-Bu_4NBF_4 as a supporting electrolyte with scan rates of 20–200 mV s^{-1} in a glovebox filled with argon at ambient temperature. Gel permeation liquid chromatography (GPLC) was performed on an LC-918 (Japan Analytical Industry Co., Ltd.) equipped with JAIGEL 1H and 2H columns (eluent: toluene). Preparative thin-layer chromatography (PTLC) and wet column chromatography were performed with Merck Kieselgel 60 PF254 and Nacalai Tesque Silica Gel 60, respectively. All melting points were determined on a Yanaco micro melting point apparatus and were uncorrected. Elemental analyses were carried out at the Microanalytical Laboratory of the Institute for Chemical Research, Kyoto University.

Reagents. 9-Bromoanthracene (TCI), 9,10-dibromoanthracene (TCI), n-butyllithium (Tosoh Finechem; 15.0 wt% in hexane), and hydrogen chloride (Aldrich; 2.0 M solution in diethyl ether), elemental selenium (Kanto; gray selenium) were used as received. 1,8-Diazabicyclo[5.4.0]undec-7-ene (DBU) and 2,3-dimethyl-1,3-butadiene were distilled from sodium hydroxide and sodium borohydride prior to use, respectively. $Cr(CO)_6$ was sublimed prior to use. Elemental sulfur, maleic

anhydride, *N*-phenylmaleimide, fumaronitrile, and anthracene were recrystallized from benzene, benzene, cyclohexane, benzene/hexane, and toluene, respectively. Chlorobis(diethylamino)phosphine,[59] 2,4,6-tris[bis(trimethylsilyl)methyl]phenylphosphine, $TbtPH_2$ (**3a**),[12e] 2,6-bis[bis(trimethylsilyl)methyl]-4-[tris(trimethylsilyl)methyl]phenylphosphine, $BbtPH_2$ (**3b**),[12h] tributylphosphine telluride,[60] maleonitrile,[61] and BbtP=PBbt[4f] were prepared according to reported procedures.

Preparation of 9-Anthrylbis(diethylamino)phosphine (6). To a solution of 9-bromoanthracene (5.14 g, 20.0 mmol) in diethyl ether (150 mL) was added *n*-butyllithium (1.50 M *n*-hexane solution, 14.7 mL, 22.0 mmol) at −78 °C.[62] The reaction mixture was stirred at 0 °C for 1 h, and cooled to −78 °C. After chlorobis(diethylamino)phosphine (5.05 mL, 24.0 mmol) was added to the solution at −78 °C, the reaction mixture was allowed to warm to room temperature and was stirred for 15 h. After the solvent was evaporated under reduced pressure, *n*-hexane was added to the residue, and then the mixture was filtered through Celite®. The solvent of the filtrate was removed to afford crude 9-anthrylbis(diethylamino)phosphine (**6**, 8.05 g, quant. If pure) as a deep red oil. The obtained mixture was used for the next reaction without further purification. **6**: ^{1}H NMR (400 MHz, C_6D_6, r.t.): δ 0.92 (t, $^3J_{HH} = 7.1$ Hz, 12H, CH_3), 2.98 (dq, $^3J_{HP} = 9.1$ Hz, $^3J_{HH} = 7.1$ Hz, 8H, CH_2), 7.28 (ddd, $^3J_{HH} = 8.7$, 7.6 Hz, $^4J_{HH} = 0.5$ Hz, 2H, Anth-3,6), 7.35 (ddd, $^3J_{HH} = 9.1$, 7.6 Hz, $^4J_{HH} = 1.5$ Hz, 2H, Anth-2,7), 7.81 (ddd, $^3J_{HH} = 8.7$ Hz, $^4J_{HH} = 1.5$ Hz, $^5J_{HH} = 0.7$ Hz, 2H, Anth-4,5), 8.18 (s, 1H, Anth-10), 9.47 (dddd, $^3J_{HH} = 9.0$ Hz, $^4J_{HP} = 3.1$ Hz, $^4J_{HH} = 0.5$ Hz, $^5J_{HH} = 0.7$ Hz, 2H, Anth-1,8); ^{13}C{^{1}H} NMR (100 MHz, C_6D_6, r.t.): δ 14.37 (d, $^3J_{CP} = 4.1$ Hz, CH_3), 44.29 (d, $^2J_{CP} = 19.0$ Hz, CH_2), 124.66 (d, $^4J_{CP} = 2.9$ Hz, Anth-2,7), 124.91 (Anth-3,6), 127.52 (d, $^3J_{CP} = 19.8$ Hz, Anth-1,8), 129.33 (d, $^4J_{CP} = 1.7$ Hz, Anth-4,5), 129.47 (d, $^4J_{CP} = 2.1$ Hz, Anth-10), 131.96 (Anth-4a,10a), 134.73 (d, $^2J_{CP} = 12.8$ Hz, Anth-8a,9a), 134.93 (d, $^1J_{CP} = 39.6$ Hz, Anth-9); ^{31}P NMR (121 MHz, C_6D_6, r.t.): δ 102.7. HRMS (EI) *m/z*, found: 352.2075 ([M]$^+$), calcd for $C_{22}H_{29}N_2P$ ([M]$^+$): 352.2068.

Preparation of 9-Anthryldichlorophosphine (4)[63] (CAS 141982–25-4). To a solution of 9-anthrylbis(diethylamino)-phosphine (**6**, 8.05 g, ca. 20 mmol) in diethyl ether (80 mL) was added hydrogen chloride (2.0 M diethyl ether solution, 60 mL, 120 mmol) at 0 °C. After stirring at room temperature for 1 h, the solvent was removed under reduced pressure. Benzene was added to the residue, and then the mixture was filtered through Celite®. After removal of the solvent from the filtrate, the residue was reprecipitated from hexane/benzene to afford 9-anthryldichlorophosphine (**4**, 3.39 g, 12.1 mmol, 61% from 9-bromoanthracene). **4**: yellow solids, ^{1}H NMR (300 MHz, C_6D_6, r.t.): δ 7.12 (ddd, $^3J_{HH} = 8.5$, 6.5 Hz, $^4J_{HH} = 0.9$ Hz, 2H, Anth-3,6), 7.23 (ddd, $^3J_{HH} = 9.1$, 6.5 Hz, $^4J_{HH} = 1.5$ Hz, 2H, Anth-2,7), 7.60 (ddd, $^3J_{HH} = 8.5$ Hz, $^4J_{HH} = 1.5$ Hz, $^5J_{HH} = 0.7$ Hz, 2H, Anth-4,5), 8.04 (s, 1H, Anth-10), 9.17 (dddd, $^3J_{HH} = 9.1$ Hz, $^4J_{HP} = 2.9$ Hz, $^4J_{HH} = 0.9$ Hz, $^5J_{HH} = 0.7$ Hz, 2H, Anth-1,8); ^{13}C{^{1}H} NMR (75 MHz, C_6D_6, r.t.): δ 125.47 (d, $^5J_{CP} = 1.9$ Hz, Anth-3,6), 125.86 (d, $^3J_{CP} = 34.6$ Hz, Anth-1,8), 127.71 (d, $^4J_{CP} = 3.7$ Hz, Anth-2,7), 129.21 (d, $^1J_{CP} = 74.0$ Hz, Anth-9), 129.84 (d, $^4J_{CP} = 1.2$ Hz, Anth-4,5), 131.31 (d, $^3J_{CP} = 4.3$ Hz, Anth-4a,10a), 134.43 (d, $^2J_{CP} = 21.6$ Hz, Anth-8a,9a), 135.47 (Anth-10); ^{31}P NMR (121 MHz, C_6D_6, r.t.): δ 159.5. HRMS (EI) found: *m/z* 277.9824 ([M]$^+$), 279.9779 ([M]$^+$), calcd for $C_{14}H_9{}^{35}Cl_2P$ ([M]$^+$): 277.9819, $C_{14}H_9{}^{35}Cl^{37}ClP$ ([M]$^+$): 279.9791.

Preparation of 9,10-Bis[bis(diethylamino)phosphino]-anthracene (7). To a suspension of 9,10-dibromoanthracene (2.02 g, 6.01 mmol) in diethyl ether (30 mL) was added *n*-butyllithium (1.45 M *n*-hexane solution, 8.69 mL, 12.6 mmol) dropwise at 0 °C.[34a,64] The reaction mixture was stirred at 0 °C for 40 min. After chlorobis(diethylamino)phosphine (2.78 mL, 13.2 mmol) was added at 0 °C, the reaction mixture was allowed to warm to room temperature, and was stirred for 12 h. After the solvents were removed under reduced pressure, *n*-hexane was added to the residue, and then the mixture was filtered through Celite®. The solvent of the filtrate was removed to afford a crude mixture containing 9,10-bis[bis(diethylamino)phosphino]anthracene (**7**, 3.53 g) as a deep red oil. The obtained mixture was used for the next reaction without further purification. **7**: ^{1}H NMR (300 MHz, C_6D_6, r.t.): δ 0.94 (t, $^3J_{HH} = 7.1$ Hz, 24H, CH_3), 2.86–3.02 (m, 16H, CH_2), 7.21–7.26 (m, 4H, Anth-2,3,6,7), 9.01–9.05 (m, 4H, Anth-1,4,5,8); ^{13}C{^{1}H} NMR (75 MHz, C_6D_6, r.t.): δ 14.64 ($^3J_{CP} = 1.9$ Hz, CH_3), 44.66–45.08 (m, CH_2), 123.27 (Anth-2,3,6,7), 126.98 (dd, $^3J_{CP} = 8.6$ Hz, $^4J_{CP} = 8.6$ Hz, Anth-1,4,5,8), 133.76 (dd, $^2J_{CP} = 4.0$ Hz, $^3J_{CP} = 4.0$ Hz, Anth-4a,10a and -8a,9a), 135.97 (dd, $^1J_{CP} = 32.7$ Hz, $^4J_{CP} = 9.9$ Hz, Anth-9,10); ^{31}P NMR (121 MHz, C_6D_6, r.t.): δ 100.7. HRMS (EI) *m/z*, found: 526.3361 ([M]$^+$), calcd for $C_{30}H_{48}N_4P_2$ ([M]$^+$): 526.3354.

Preparation of 9,10-Bis(dichlorophosphino)anthracene (5). To a solution of 9,10-bis[bis(diethylamino)phosphino]-anthracene (**7**, 3.53 g) in diethyl ether (90 mL) was added hydrogen chloride (2.0 M diethyl ether solution, 36 mL, 72 mmol) at 0 °C. After stirring at 0 °C for 30 min, the suspension was separated by filtration and washed with hexane. The solid was dissolved in benzene, and the suspension was filtered through Celite® to remove the inorganic salt. The solvent of the filtrate was removed under reduced pressure to afford 9,10-bis(dichlorophosphino)anthracene (**5**, 578 mg, 1.52 mmol). The mother liquid was removed under reduced pressure, and the residue was filtered through Celite® with benzene. After removal of the solvent from the filtrate, the residue was washed with hexane and was reprecipitated from hexane/benzene to afford 9,10-bis(dichlorophosphino)anthracene (**5**, 360 mg, 0.947 mmol). Total (938 mg, 2.47 mmol, 41% from 9,10-dibromoanthracene) **5**: yellow solid, mp: 192 °C (decomp.). ^{1}H NMR (400 MHz, C_6D_6, r.t.): δ 7.08–7.12 (m, 4H, Anth-2,3,6,7), 9.04–9.09 (m, 4H, Anth-1,4,5,8); ^{13}C{^{1}H} NMR (100 MHz, C_6D_6, r.t.): δ 126.73 (dd, $^3J_{CP} = 36.5$ Hz, $^4J_{CP} = 1.1$ Hz, Anth-1,4,5,8), 127.13 (dd, $^4J_{CP} = 3.8$ Hz, $^5J_{CP} = 2.2$ Hz, Anth-2,3,6,7), 133.17 (dd, $^2J_{CP} = 19.6$ Hz, $^3J_{CP} = 2.6$ Hz, Anth-4a,10a and -8a,9a), 137.24 (dd, $^1J_{CP} = 78.4$ Hz, $^4J_{CP} = 0.9$ Hz, Anth-9,10); ^{31}P NMR (121 MHz, C_6D_6, r.t.): δ 155.7. HRMS (EI) *m/z*, found: 377.8838 ([M]$^+$), 379.8828 ([M]$^+$), 381.8776 ([M]$^+$), calcd for $C_{14}H_8{}^{35}Cl_4P_2$ ([M]$^+$): 377.8855, $C_{14}H_8{}^{35}Cl_3{}^{37}ClP_2$ ([M]$^+$): 379.8826, $C_{14}H_8{}^{35}Cl_2{}^{37}Cl_2P_2$ ([M]$^+$): 381.8796. Anal. Found: C, 44.54; H, 2.23%. Calcd for $C_{14}H_8Cl_4P_2$: C, 44.25; H, 2.12%.

Synthesis of TbtP=P(9-Anth) (1a). In a glovebox filled with argon, DBU (224 μL, 1.50 mmol) was added to a toluene

solution (15 mL) of $TbtPH_2$ (**3a**, 351 mg, 0.600 mmol) and 9-anthryldichlorophosphine (**4**, 201 mg, 0.720 mmol) at room temperature. After stirring at room temperature for 21 h, the reaction mixture was filtered through Celite® with toluene. The solvent of the filtrate was removed under reduced pressure, and then the residue was washed with benzene to afford 9-anthryldiphosphene **1a** (340 mg, 0.430 mmol, 71%). **1a**: red crystals, mp: 242 °C (decomp.). ^{1}H NMR (400 MHz, C_6D_6, r.t.): δ 0.23 (s, 18H, $SiMe_3$), 0.29 (s, 36H, $SiMe_3$), 1.58 (s, 1H, Tbt-*p*-benzyl), 2.65 (br s, 1H, Tbt-*o*-benzyl), 2.77 (br s, 1H, *o*-benzyl), 6.76 (br s, 1H, Tbt-*m*-aromH), 6.88 (br s, 1H, Tbt-*m*-aromH), 7.27 (ddd, $^3J_{HH} = 8.5$, 6.5 Hz, $^4J_{HH} = 0.6$ Hz, 2H, Anth-3,6), 7.44 (ddd, $^3J_{HH} = 9.0$, 6.5 Hz, $^4J_{HH} = 1.2$ Hz, 2H, Anth-2,7), 7.80 (ddd, $^3J_{HH} = 8.5$ Hz, $^4J_{HH} = 1.2$ Hz, $^5J_{HH} = 0.5$ Hz, 2H, Anth-4,5), 8.18 (s, 1H, Anth-10), 8.61 (d, $^3J_{HH} = 9.0$ Hz, 2H, Anth-1,8); ^{13}C{^{1}H} NMR (100 MHz, C_6D_6, r.t.): δ 0.91 ($SiMe_3$), 1.36 ($SiMe_3$), 30.87 (Tbt-*p*-benzyl), 32.04 (Tbt-*o*-benzyl), 32.38 (Tbt-*o*-benzyl), 122.73 (Tbt-arom-*m*-CH), 125.31 (Anth-3,6), 125.37 (Anth-2,7), 127.30 (Tbt-arom-*m*-CH), 128.63 (d, $^3J_{CP} = 6.6$ Hz, Anth-1,8), 129.59 (Anth-4,5), 129.64 (Anth-10), 132.27 (Anth-4a,10a), 133.53 (Anth-8a,9a), 135.53 (d, $^1J_{CP} = 42.1$ Hz, Tbt-C_{ipso}), 139.91 (d, $^1J_{CP} = 52.8$ Hz, Anth-9), 145.33 (Tbt-arom-*p*-C), 145.94 (Tbt-arom-*o*-C); ^{31}P NMR (121 MHz, C_6D_6, r.t.): δ 526.2, 584.3 (d, $^1J_{PP} = 581$ Hz). HRMS (EI) *m*/*z*, found: 790.3404 ($[M]^+$), calcd for $C_{41}H_{68}Si_6P_2$ ($[M]^+$): 790.3412. Anal. Found: C, 61.94; H, 8.77%. Calcd for $C_{41}H_{68}Si_6P_2$: C, 62.22; H, 8.66%. UV–vis (hexane): λ_{max} 530 (ε 780), 438 (sh, 1300), 400 (14000), 380 (15000), 361 (9500), 310 nm (7200).

Synthesis of BbtP=P(9-Anth) (1b). In a glovebox filled with argon, DBU (93 µL, 0.62 mmol) was added to a toluene (10 mL) solution of $BbtPH_2$ (**3b**, 165 mg, 0.251 mmol) and 9-anthryldichlorophosphine (**4**, 83.7 mg, 0.300 mmol) at room temperature. After stirring at room temperature for 2 h, the reaction mixture was filtered through Celite® with toluene. The solvent of the filtrate was removed under reduced pressure, and then the residue was washed with cooled hexane to afford 9-anthryldiphosphene **1b** (167 mg, 0.193 mmol, 77%). **1b**: red crystals, mp: 229 °C (decomp.). ^{1}H NMR (400 MHz, C_6D_6, r.t.): δ 0.31 (s, 36H, $SiMe_3$), 0.43 (s, 27H, $SiMe_3$), 2.87 (s, 2H, Bbt-*o*-benzyl), 7.19 (s, 2H, Bbt-*m*-aromH), 7.28 (ddd, $^3J_{HH} = 8.5$, 6.5 Hz, $^4J_{HH} = 1.0$ Hz, 2H, Anth-3,6), 7.46 (ddd, $^3J_{HH} = 8.7$, 6.5 Hz, $^4J_{HH} = 1.4$ Hz, 2H, Anth-2,7), 7.80 (d, $^3J_{HH} = 8.5$ Hz, 2H, Anth-4,5), 8.18 (s, 1H, Anth-10), 8.62 (d, $^3J_{HH} = 8.7$ Hz, 2H, Anth-1,8); ^{13}C{^{1}H} NMR (100 MHz, C_6D_6, r.t.): δ 1.78 ($SiMe_3$), 5.60 ($SiMe_3$), 22.49 (Bbt-*p*-benzyl), 33.59 (Bbt-*o*-benzyl), 125.38 (Anth-3,6), 125.44 (Anth-2,7), 127.38 (Bbt-arom-*m*-CH), 128.72 (d, $^3J_{CP} = 7.4$ Hz, Anth-1,8), 129.61 (Anth-4,5), 129.79 (Anth-10), 132.26 (Anth-4a,10a), 133.54 (d, $^2J_{CP} = 4.9$ Hz, Anth-8a,9a), 137.38 (br d, $^1J_{CP} = 44.5$ Hz, Bbt-C_{ipso}), 139.70 (br d, $^1J_{CP} = 58.6$ Hz, Anth-9), 145.64 (Bbt-arom-*o*-C), 146.85 (Bbt-arom-*p*-C); ^{31}P NMR (121 MHz, C_6D_6, r.t.): δ 521.9, 586.8 (AB quartet, $^1J_{PP} = 584$ Hz). HRMS (FAB) *m*/*z*, found: 863.3900 ($[M + H]^+$), calcd for $C_{44}H_{77}P_2Si_7$ ($[M + H]^+$): 863.3885. Anal. Found: C, 61.29; H, 8.94%. Calcd for $C_{44}H_{76}P_2Si_7$: C, 61.19; H, 8.87%. UV–vis (hexane): λ_{max} 532 (ε 790), 437 (sh, 1200), 400 (13000), 380 (14000), 361 (9100), 314 nm (6500).

Synthesis of TbtP=P($C_{14}H_8$)P=PTbt (2a, $C_{14}H_8$ = 9,10-Anthrylene). In a glovebox filled with argon, DBU (0.50 M THF solution, 3.5 mL, 1.75 mmol) was added dropwise to a THF (12 mL) solution of $TbtPH_2$ (**3a**, 468 mg, 0.800 mmol) and 9,10-bis(dichlorophosphino)anthracene (**5**, 182 mg, 0.479 mmol) at room temperature. After stirring at room temperature for 4.5 h, the solvent was removed under reduced pressure. The reaction mixture was filtered through Celite® with toluene, and then the solvent of the filtrate was removed under reduced pressure. The residue was washed with cooled hexane to afford bisdiphosphene **2a** (114 mg, 0.0814 mmol, 20%). **2a**: red crystals, mp: 279 °C (decomp.). ^{1}H NMR (300 MHz, C_6D_6, r.t.): δ 0.25 (s, 36H, $SiMe_3$), 0.31 (s, 72H, $SiMe_3$), 1.60 (s, 2H, Tbt-*p*-benzyl), 2.67 (br s, 2H, Tbt-*o*-benzyl), 2.78 (br s, 2H, Tbt-*o*-benzyl), 6.78 (br s, 2H, Tbt-*m*-aromH), 6.88 (br s, 2H, Tbt-*m*-aromH), 7.44–7.48 (m, 4H, Anth-2,3,6,7), 8.66–8.70 (m, 4H, Anth-1,4,5,8); ^{31}P NMR (121 MHz, C_6D_6, 50 °C): δ 528.8, 585.2 (AB quartet, $^1J_{PP} = 588$ Hz). HRMS (FAB) *m*/*z*, found: 1403.6118 ($[M + H]^+$), calcd for $C_{68}H_{127}P_4Si_{12}$ ($[M + H]^+$): 1403.6119. Anal. Found: C, 58.01; H, 9.09%. Calcd for $C_{68}H_{126}P_4Si_{12}$: C, 58.14; H, 9.04%. UV–vis (hexane): λ_{max} 538 (ε 2500), 426 (25000), 403 (23000), 382 (sh, 13000), 364 (sh, 8300), 312 nm (14000). The ^{13}C NMR data could not be obtained due to its extremely low solubility in organic solvents.

Synthesis of BbtP=P($C_{14}H_8$)P=PBbt (2b, $C_{14}H_8$ = 9,10-Anthrylene). In a glovebox filled with argon, DBU (0.50 M THF solution, 3.5 mL, 1.75 mmol) was added dropwise to a THF (12 mL) solution of $BbtPH_2$ (**3b**, 526 mg, 0.800 mmol) and 9,10-bis(dichlorophosphino)anthracene (**5**, 182 mg, 0.479 mmol) at room temperature. After stirring at room temperature for 3 h, the solvent was removed under reduced pressure. The reaction mixture was filtered through Celite® with toluene, and then the solvent of the filtrate was removed under reduced pressure. The residue was washed with cooled hexane and recrystallized from THF/hexane at −40 °C to afford bisdiphosphene **2b** (136 mg, 0.0880 mmol, 22%). **2b**: deep red crystals, mp: 288 °C (decomp.). ^{1}H NMR (400 MHz, C_6D_6, r.t.): δ 0.34 (s, 72H, $SiMe_3$), 0.45 (s, 54H, $SiMe_3$), 2.88 (s, 4H, Bbt-*o*-benzyl), 7.21 (s, 4H, Bbt-*m*-aromH), 7.48–7.52 (m, 4H, Anth-2,3,6,7), 8.68–8.72 (m, 4H, Anth-1,4,5,8); ^{31}P NMR (121 MHz, C_6D_6, 50 °C): δ 522.1, 585.0 (AB quartet, $^1J_{PP} = 584$ Hz). HRMS (FAB) *m*/*z*, found: 1547.6897 ($[M + H]^+$), calcd for $C_{74}H_{143}P_4Si_{14}$ ($[M + H]^+$): 1547.6910. Anal. Found: C, 57.19; H, 9.41%. Calcd for $C_{74}H_{142}P_4Si_{14}$: C, 57.38; H, 9.24%. UV–vis (hexane): λ_{max} 542 (ε 2200), 427 (21000), 403 (20000), 383 (sh, 12000), 363 (sh, 7200), 315 nm (12000). The ^{13}C NMR data could not be obtained due to its extremely low solubility in organic solvents.

Reaction of TbtP=P(9-Anth) (1a) with [Cr(CO)$_5$(thf)]. A solution of $Cr(CO)_6$ (220 mg, 0.997 mmol) in THF (25 mL) was irradiated with a 100 W medium pressure Hg-lamp at room temperature for 3 h. The resulting orange solution of [Cr(CO)$_5$(thf)][65] (15 mL, 0.60 mmol) was added to a solution of TbtP=P(9-Anth) (**1a**, 39.6 mg, 50.0 µmol) in THF (3 mL) under dark conditions. After the reaction mixture was stirred at 30 °C for 20 h under dark conditions, the solvents were evaporated under reduced pressure. To the residue was added benzene and the suspension was purified by silica gel column chromatography (SiO_2/benzene) under air. The solvent was removed under reduced pressure, and then the residue was

washed with hexane to afford (*E*)-9-anthryldiphosphene–$Cr(CO)_5$ complex **13** (47.2 mg, 48.0 μmol, 96%). This compound is light sensitive. **13**: red-orange crystals, mp: 166 °C (decomp.). ^{1}H NMR (400 MHz, $CDCl_3$, r.t.): δ −0.06 (s, 18H, $SiMe_3$), 0.10 (s, 18H, $SiMe_3$), 0.41 (s, 18H, $SiMe_3$), 1.44 (s, 1H, Tbt-*p*-benzyl), 2.39 (br s, 1H, Tbt-*o*-benzyl), 2.47 (br s, 1H, Tbt-*o*-benzyl), 6.50 (br s, 1H, Tbt-*m*-aromH), 6.67 (br s, 1H, Tbt-*m*-aromH), 7.55–7.62 (m, 4H, Anth-2,3,6,7), 8.11 (d, $^3J_{HH} = 8.2$ Hz, 2H, Anth-4,5), 8.47 (d, $^3J_{HH} = 8.5$ Hz, 2H, Anth-1,8), 8.62 (s, 1H, Anth-10); ^{13}C{^{1}H} NMR (100 MHz, $CDCl_3$, r.t.): δ 0.53 ($SiMe_3$), 0.88 ($SiMe_3$), 1.20 ($SiMe_3$), 1.65 ($SiMe_3$), 2.20 ($SiMe_3$), 2.32 ($SiMe_3$), 30.91 (Tbt-*p*-benzyl), 31.12 (Tbt-*o*-benzyl), 31.45 (Tbt-*o*-benzyl), 122.86 (Tbt-arom-*m*-CH), 125.47 (Anth-3,6), 126.47 (Anth-2,7), 127.47 (Anth-1,8), 127.63 (Tbt-arom-*m*-CH), 129.48 (Anth-4,5), 130.04 (br d, $^1J_{CP} = 49.3$ Hz, Tbt-C_{ipso}), 130.59 (Anth-10), 131.48 (Anth-4a,10a), 132.05 (Anth-8a,9a), 139.78 (br d, $^1J_{CP} = 23.6$ Hz, Anth-9), 146.38 (Tbt-arom-*p*-C), 146.64 (Tbt-arom-*o*-C), 213.86 (d, $^2J_{CP} = 12.9$ Hz, *cis*-CO), 222.51 (*trans*-CO); ^{31}P NMR (121 MHz, $CDCl_3$, r.t.): δ 422.6, 519.8 (AB quartet, $^1J_{PP} = 527$ Hz). HRMS (FAB) *m*/*z*, found: 983.2662 ([M + H]$^+$), calcd for $C_{46}H_{69}CrO_5P_2Si_6$ ([M + H]$^+$): 983.2643. Anal. Found: C, 55.90; H, 6.91%. Calcd for $C_{46}H_{68}CrO_5P_2Si_6$: C, 56.18; H, 6.97%. UV–vis (hexane): λ_{max} 465 (ε 11000), 400 (10000), 378 (11000), 360 nm (9200).

Reaction of BbtP=P(9-Anth) (1b) with Elemental Sulfur (S_8). A C_6D_6 suspension (0.8 mL) of BbtP=P(9-Anth) (**1b**, 60.5 mg, 70.0 μmol) and elemental sulfur (S_8, 2.7 mg, 84 μmol as S) was degassed and sealed in an NMR tube. After stirring at room temperature for 58 h, the solvent of the reaction mixture was removed under reduced pressure. The residue was washed with hexane to afford 2-anthryl-3-Bbt-thiadiphosphirane (**14**, 43.3 mg, 48.3 μmol, 69%). **14**: yellow crystals, mp: 230 °C (decomp.). ^{1}H NMR (400 MHz, C_6D_6, r.t.): δ 0.28 (s, 18H, $SiMe_3$), 0.36 (s, 27H, $SiMe_3$), 0.44 (s, 18H, $SiMe_3$), 3.53–3.54 (m, 2H, Bbt-*o*-benzyl), 6.96 (d, $^4J_{HP} = 1.7$ Hz, 2H, Bbt-*m*-aromH), 7.16 (ddd, $^3J_{HH} = 8.5$, 6.5 Hz, $^4J_{HH} = 0.7$ Hz, 2H, Anth-3,6), 7.39 (ddd, $^3J_{HH} = 9.0$, 6.5 Hz, $^4J_{HH} = 1.2$ Hz, 2H, Anth-2,7), 7.65 (ddd, $^3J_{HH} = 8.5$ Hz, $^4J_{HH} = 0.7$ Hz, $^5J_{HH} = 0.4$ Hz, 2H, Anth-4,5), 7.98 (s, 1H, Anth-10), 9.11 (d, $^3J_{HH} = 9.0$ Hz, 2H, Anth-1,8); ^{13}C{^{1}H} NMR (100 MHz, C_6D_6, r.t.): δ 1.79 (d, $J = 2.5$ Hz, *o*-$SiMe_3$), 2.05 (*o*-$SiMe_3$), 5.74 (*p*-$SiMe_3$), 22.34 (Bbt-*p*-benzyl), 31.97 (m, Bbt-*o*-benzyl), 125.18 (Anth-3,6), 126.71 (Anth-2,7), 127.69 (Bbt-arom-*m*-CH), 127.94 (pseudotriplet, $^3J_{CP} = 5.8$ Hz, $^4J_{CP} = 5.8$ Hz, Anth-1,8), 129.90 (Anth-4,5), 130.88 (Anth-10), 131.64 (Anth-4a,10a), 133.81 (dd, $^1J_{CP} = 64$ Hz, $^2J_{CP} = 10$ Hz, Bbt-arom-*ipso*-C), 134.29 (dd, $^1J_{CP} = 69$ Hz, $^2J_{CP} = 8.2$ Hz, Anth-9), 134.77 (br d, $^2J_{CP} = 7.4$ Hz, Anth-8a,9a), 146.55 (Bbt-arom-*p*-C), 148.91 (d, $^2J_{CP} = 9.1$ Hz, Bbt-arom-*o*-C); ^{31}P NMR (121 MHz, C_6D_6, r.t.): δ −81.9, −80.3 (AB quartet, $^1J_{PP} = 227$ Hz). HRMS (FAB) *m*/*z*, found: 895.3610 ([M + H]$^+$), calcd for $C_{44}H_{77}P_2SSi_7$ ([M + H]$^+$): 895.3606. Anal. Found: C, 58.93; H, 8.69%. Calcd for $C_{44}H_{76}P_2SSi_7$: C, 59.00; H, 8.55%.

Reaction of BbtP=P(9-Anth) (1b) with Elemental Selenium. A C_6D_6 suspension (0.8 mL) of BbtP=P(9-Anth) (**1b**, 60.5 mg, 70.0 μmol) and elemental selenium (gray selenium, 27.6 mg, 0.350 mmol) was degassed and sealed in an NMR tube. After heating at 80 °C for 6 h, the reaction mixture was filtered through Celite® with benzene. The solvent of the filtrate was removed under reduced pressure, and the residue was washed with hexane to afford 2-anthryl-3-Bbt-selenadiphosphirane (**15**, 55.6 mg, 59.0 μmol, 84%). **15**: yellow crystals, mp: 224 °C (decomp.). ^{1}H NMR (400 MHz, C_6D_6, r.t.): δ 0.28 (s, 18H, $SiMe_3$), 0.36 (s, 27H, $SiMe_3$), 0.41 (s, 18H, $SiMe_3$), 3.66–3.68 (m, 2H, Bbt-*o*-benzyl), 6.96 (d, $^4J_{HP} = 2.2$ Hz, 2H, Bbt-*m*-aromH), 7.16 (dd, $^3J_{HH} = 8.0$ Hz, $^3J_{HH} = 6.5$ Hz, 2H, Anth-3,6), 7.38 (ddd, $^3J_{HH} = 9.0$ Hz, $^3J_{HH} = 6.5$ Hz, $^4J_{HH} = 1.0$ Hz, 2H, Anth-2,7), 7.63 (d, $^3J_{HH} = 8.0$ Hz, 2H, Anth-4,5), 7.94 (s, 1H, Anth-10), 9.16 (d, $^3J_{HH} = 9.0$ Hz, 2H, Anth-1,8); ^{13}C{^{1}H} NMR (100 MHz, C_6D_6, r.t.): δ 1.72 (d, $J = 2.4$ Hz, *o*-$SiMe_3$), 2.18 (*o*-$SiMe_3$), 5.74 (*p*-$SiMe_3$), 22.36 (Bbt-*p*-benzyl), 32.14 (pseudotriplet, $^3J_{CP} = 5.7$ Hz, $^4J_{CP} = 5.7$ Hz, Bbt-*o*-benzyl), 125.11 (Anth-3,6), 126.49 (d, $^4J_{CP} = 2.5$ Hz, Anth-2,7), 127.74 (Bbt-arom-*m*-CH), 128.37 (pseudotriplet, $^3J_{CP} = 8.1$ Hz, $^4J_{CP} = 8.1$ Hz, Anth-1,8), 129.91 (Anth-4,5), 131.00 (br d, $^4J_{CP} = 2.1$ Hz, Anth-10), 131.60 (Anth-4a,10a), 132.91 (d, $^1J_{CP} = 77$ Hz, Bbt-C_{ipso}), 133.89 (d, $^1J_{CP} = 80$ Hz, Anth-9), 134.97 (br d, $^2J_{CP} = 8.2$ Hz, Anth-8a,9a), 146.60 (Bbt-arom-*p*-C), 149.24 (d, $^2J_{CP} = 12$ Hz, Bbt-arom-*o*-C); ^{31}P NMR (121 MHz, C_6D_6, r.t.): δ −70.2 (AB quartet, $^1J_{PP} = 239.5$ Hz, $^1J_{PSe} = 125.0$ Hz), −63.5 (AB quartet, $^1J_{PP} = 239.5$ Hz, $^1J_{PSe} = 123.3$ Hz). ^{77}Se NMR (75 MHz, C_6D_6, 50 °C): δ 72.0 (pseudotriplet, $^1J_{SeP} = 123$ Hz). HRMS (FAB) *m*/*z*, found: 943.3054 ([M + H]$^+$), calcd for $C_{44}H_{77}P_2{}^{80}SeSi_7$ ([M + H]$^+$): 943.3051. Anal. Found: C, 56.18; H, 8.09%. Calcd for $C_{44}H_{76}P_2SeSi_7$: C, 56.07; H, 8.13%.

Reaction of BbtP=P(9-Anth) (1b) with (*n*-Bu)$_3$P=Te. A THF suspension (0.6 mL) of BbtP=P(9-Anth) (**1b**, 60.5 mg, 70.0 mmol) and (*n*-Bu)$_3$P=Te (231 mg, 0.700 mmol) was degassed and sealed in an NMR tube. After heating the mixture at 80 °C for 98 h, the bright red color of the reaction mixture turned deep red and yellow powder was precipitated. After the signals for **1b** almost disappeared, the yellow suspension was separated by filtration and washed with hexane. The yellow solid was dissolved in toluene and filtered through a glass filter to remove the inorganic salt. The solvent of the filtrate was removed under reduced pressure to afford 1,2-dianthryl-3-Bbt-triphosphirane (**20**, 25.7 mg, 24.0 μmol, 68%) as yellow crystals. The solvent of the mother liquid was removed under reduced pressure, and the residue was separated by GPLC to afford BbtP=PBbt (**21**, 16.7 mg, 12.7 μmol, 73%) as red crystals. **20**: yellow crystals, mp 263 °C (decomp.). ^{1}H NMR (300 MHz, C_6D_6, 40 °C): δ 0.39 (s, 36H), 0.43 (s, 27H), 4.07 (s, 2H), 6.82 (br s, 4H), 6.89 (pseudotriplet, $^3J_{HH} = 6.8$ Hz, 4H), 7.07 (d, $^4J_{HP} = 2.5$ Hz, 2H), 7.26 (d, $^3J_{HH} = 8.9$ Hz, 4H), 7.46 (s, 2H), 9.11 (d, $^3J_{HH} = 8.5$ Hz, 4H); ^{31}P NMR (121 MHz, C_6D_6, r.t.): δ −92.9, −127.4 (A_2B spin pattern, $^1J_{PP} = 188$ Hz). HRMS (FAB) *m*/*z*, found: 1071.4335 ([M + H]$^+$), calcd for $C_{58}H_{86}P_3Si_7$ ([M + H]$^+$): 1071.4327. Anal. Found: C, 64.15; H, 8.00%. Calcd for $C_{58}H_{85}P_3Si_7$: C, 64.99; H, 7.99%. The signals observed in the ^{13}C NMR spectrum could not be assigned due to the complication.

Reaction of BbtP=P(9-Anth) (1b) with 2,3-Dimethyl-1,3-butadiene. A C_6D_6 suspension (0.9 mL) of BbtP=P(9-Anth) (**1b**, 51.8 mg, 60.0 μmol) and 2,3-dimethyl-1,3-butadiene (68 μL, 49 mg, 0.60 mmol) was degassed and sealed in an NMR tube. After heating at 60 °C for 15 h, the solvent was

removed under reduced pressure. The residue was separated by GPLC to afford 1,2-diphosphacyclohex-4-ene derivative **29** (37.9 mg, 40.1 μmol, 67%). **29**: yellow crystals, mp: 198 °C (decomp.). ^{1}H NMR (400 MHz, C_6D_{12}, 50 °C): δ −0.33 (br s, 18H), 0.15 (s, 18H), 0.23 (s, 27H), 1.65 (d, $J = 2.9$ Hz, 3H), 2.10 (s, 3H), 2.40 (dt, $J = 12.6$, 10.2 Hz, 1H), 2.51 (dd, $J = 15.4$, 2.8 Hz, 1H), 3.19–3.31 (m, 1H), 3.36 (br s, 2H), 3.41–3.45 (m, 1H), 6.71 (s, 2H), 7.26–7.35 (m, 4H), 7.82 (d, $^3J_{HH} = 8.5$ Hz, 2H), 8.29 (s, 1H), 9.39 (d, $^3J_{HH} = 8.0$ Hz, 2H); ^{13}C{^{1}H} NMR (100 MHz, C_6D_{12}, 50 °C): δ 1.83 (CH_3), 2.24 (CH_3), 5.93 (CH_3), 20.03 (CH_3), 21.40 (CH_3), 22.95, 29.76 (d, $^3J_{CP} = 9.1$ Hz, CH), 29.96 (d, $^3J_{CP} = 9.1$ Hz, CH), 31.74 (dd, $^1J_{CP} = 22.3$ Hz, $^2J_{CP} = 9.1$ Hz, CH_2), 33.24 (dd, $^1J_{CP} = 20.6$ Hz, $^2J_{CP} = 4.9$ Hz, CH_2), 125.12 (CH), 125.48 (CH), 127.80 (dd, $^2J_{CP} = 4.5$ Hz, $^3J_{CP} = 2.1$ Hz), 128.14 (CH), 128.57 (d, $^1J_{CP} = 21.0$ Hz, $^2J_{CP} = 2.9$ Hz), 129.51 (CH), 130.43 (dd, $^3J_{CP} = 20.2$ Hz, $^4J_{CP} = 14.4$ Hz, CH), 130.81 (d, $^2J_{CP} = 4.9$ Hz), 131.24 (CH), 132.86 (dd, $^3J_{CP} = 2.0$ Hz, $^4J_{CP} = 2.0$ Hz), 133.03 (d, $^1J_{CP} = 28.0$ Hz), 138.03 (dd, $^2J_{CP} = 9.5$ Hz, $^3J_{CP} = 4.5$ Hz), 146.75, 153.52; ^{31}P NMR (121 MHz, C_6D_6, r.t.): δ −58.2, −57.4 (AB quartet, $^1J_{PP} = 208$ Hz). HRMS (FAB) m/z, found: 945.4689 ([M + H]$^+$), calcd for $C_{50}H_{87}P_2Si_7$ ([M + H]$^+$): 945.4668. Anal. Found: C, 63.38; H, 9.38%. Calcd for $C_{50}H_{86}P_2Si_7$: C, 63.50; H, 9.17%.

Reaction of BbtP=P(9-Anth) (1b) with Maleic Anhydride (30a). A C_6D_6 suspension (0.9 mL) of BbtP=P(9-Anth) (**1b**, 51.8 mg, 60.0 μmol) and maleic anhydride (**30a**, 17.8 mg, 0.182 mmol) was degassed and sealed in an NMR tube. After heating at 120 °C for 14 h, the reaction mixture was filtered through Celite® with toluene. The solvent of the filtrate was removed under reduced pressure, and the residue was separated by GPLC to afford maleic anhydride adduct **31a** (49.1 mg, 51.1 μmol, 85%). **31a**: orange crystals, mp: 235 °C (decomp.). ^{1}H NMR (400 MHz, C_6D_6, r.t.): δ 0.368 (s, 18H), 0.370 (s, 18H), 0.45 (s, 27H), 2.76 (dd, $^3J_{HH} = 9.1$, 3.3 Hz, 1H), 2.85 (s, 2H), 4.53 (d, $^3J_{HH} = 3.3$ Hz, 1H), 4.55 (br d, $^3J_{HH} = 9.1$ Hz, 1H), 6.77 (ddd, $^3J_{HH} = 7.5$, 7.3 Hz, $^4J_{HH} = 1.2$ Hz, 1H), 6.84 (ddd, $^3J_{HH} = 7.5$, 7.3 Hz, $^4J_{HH} = 1.5$ Hz, 1H), 6.92 (ddd, $^3J_{HH} = 7.3$, 7.3 Hz, $^4J_{HH} = 1.0$ Hz, 1H), 6.97 (dd, $^3J_{HH} = 7.3$ Hz, $^5J_{HH} = 1.5$ Hz, 1H), 7.06 (dd, $^3J_{HH} = 7.3$ Hz, $^4J_{HH} = 1.2$ Hz, 1H), 7.14 (ddd, $^3J_{HH} = 7.8$, 7.3 Hz, $^4J_{HH} = 1.5$ Hz, 1H),[66] 7.26 (s, 2H), 7.74 (d, $^3J_{HH} = 7.8$ Hz, 1H), 7.84 (d, $^3J_{HH} = 7.3$ Hz, 1H); ^{13}C{^{1}H} NMR (100 MHz, C_6D_6, r.t.): δ 1.83 (CH_3), 1.88 (CH_3), 5.67 (CH_3), 22.61, 33.53 (CH), 46.55 (CH), 49.94 (CH), 52.85 (d, $^2J_{CP} = 15.7$ Hz, CH), 56.78 (d, $^1J_{CP} = 66.8$ Hz), 124.60 (CH), 125.60 (d, $^3J_{CP} = 23.9$ Hz, CH), 125.90 (CH), 126.28 (CH), 127.00 (CH), 127.32 (CH), 127.68 (CH × 2), 127.86 (CH), 134.85 (br d, $^1J_{CP} = 34.6$ Hz), 138.85, 141.13 (br d, $^2J_{CP} = 10.7$ Hz), 142.58, 143.98, 146.39, 147.36, 169.79; ^{31}P NMR (121 MHz, C_6D_6, r.t.): δ 520.3, 571.2 (AB quartet, $^1J_{PP} = 583$ Hz). HRMS (FAB) m/z, found: 961.3905 ([M + H]$^+$), calcd for $C_{48}H_{79}O_3P_2Si_7$ ([M + H]$^+$): 961.3889. Anal. Found: C, 59.67; H, 8.42%. Calcd for $C_{48}H_{78}O_3P_2Si_7$: C, 59.95; H, 8.18%. UV–vis (hexane): λ_{max} 487 (ε 420), 370 (sh, 2100), 323 nm (6900).

Reaction of BbtP=P(9-Anth) (1b) with *N*-Phenylmaleimide (30b). A C_6D_6 suspension (0.9 mL) of BbtP=P(9-Anth) (**1b**, 51.8 mg, 60.0 μmol) and *N*-phenylmaleimide (**30b**, 31.2 mg, 0.180 mmol) was degassed and sealed in an NMR tube. After heating at 120 °C for 6 h, the reaction mixture was filtered through Celite® with toluene. The solvent of the filtrate was removed under reduced pressure, and then the residue was separated by GPLC to afford *N*-phenylmaleimide adduct **31b** (53.7 mg, 51.7 μmol, 86%). **31b**: orange crystals, mp: 232 °C (decomp.). ^{1}H NMR (400 MHz, C_6D_6, r.t.): δ 0.348 (s, 18H), 0.356 (s, 18H), 0.45 (s, 27H), 2.976 (dd, $^3J_{HH} = 8.5$, 3.1 Hz, 1H), 2.982 (s, 2H), 4.60 (br d, $^3J_{HH} = 8.5$ Hz, 1H), 4.79 (d, $^3J_{HH} = 3.1$ Hz, 1H), 6.71–6.74 (m, 2H), 6.81–6.91 (m, 3H), 6.96–7.03 (m, 3H), 7.14 (d, $^3J_{HH} = 7.5$ Hz, 1H),[66] 7.16 (dd, $^3J_{HH} = 7.0$ Hz, $^4J_{HH} = 1.4$ Hz, 1H),[66] 7.23 (ddd, $^3J_{HH} = 7.5$, 7.5 Hz, $^4J_{HH} = 1.3$ Hz, 1H), 7.25 (s, 2H), 7.92 (d, $^3J_{HH} = 7.5$ Hz, 1H), 7.94 (d, $^3J_{HH} = 7.5$ Hz, 1H); ^{13}C{^{1}H} NMR (100 MHz, C_6D_6, r.t.): δ 1.83 (CH_3), 1.88 (CH_3), 5.68 (CH_3), 22.52, 33.18 (CH), 47.21 (CH), 49.36 (CH), 52.57 (d, $^2J_{CP} = 13.2$ Hz, CH), 57.05 (d, $^1J_{CP} = 64.3$ Hz), 124.68 (CH), 125.72 (d, $^3J_{CP} = 19.0$ Hz, CH), 125.81 (CH), 126.10 (CH), 126.51 (CH), 127.06 (CH), 127.19 (CH × 2), 127.26 (br, CH), 127.62 (CH), 128.27 (CH), 128.57 (CH), 132.29, 135.74 (d, $^1J_{CP} = 27.2$ Hz), 139.84, 141.58 (d, $^3J_{CP} = 4.9$ Hz), 143.39, 144.53, 146.42, 146.91, 174.55, 174.61; ^{31}P NMR (121 MHz, C_6D_6, r.t.): δ 525.8, 564.3 (AB quartet, $^1J_{PP} = 577$ Hz). HRMS (FAB) m/z, found: 1036.4352 ([M + H]$^+$), calcd for $C_{54}H_{84}NO_2P_2Si_7$ ([M + H]$^+$): 1036.4362. Anal. Found: C, 62.63; H, 8.09; N, 1.40%. Calcd for $C_{54}H_{83}NO_2P_2Si_7$: C, 62.56; H, 8.07; N, 1.35%. UV–vis (hexane): λ_{max} 484 (ε 390), 369 (sh, 2300), 328 nm (6400).

Reaction of BbtP=P(9-Anth) (1b) with 30 equiv of Fumaronitrile (30c). A C_6D_6 suspension (0.9 mL) of BbtP=P(9-Anth) (**1b**, 51.8 mg, 60.0 μmol) and fumaronitrile (**30c**, 141 mg, 1.81 mmol) was degassed and sealed in an NMR tube. After heating at 120 °C for 13 h, the starting material **1b** and fumaronitrile adduct **31c** were observed in the ratio of 3:97 as judged by the ^{1}H NMR spectra together with maleonitrile (**30d**).[67] After the reaction mixture was filtered through Celite® with toluene, the solvent of the filtrate was removed under reduced pressure. The residue was separated by GPLC and then PTLC (eluent: benzene, $R_f = 0.5$) to afford fumaronitrile adduct **31c** (47.1 mg, 50.0 μmol, 83%) **31c**: orange crystals, mp: 210 °C (decomp.). ^{1}H NMR (400 MHz, C_6D_6, r.t.): δ 0.29 (s, 18H), 0.35 (s, 18H), 0.42 (s, 27H), 2.59 (s, 2H), 2.67 (dd, $^3J_{HH} = 4.1$, 2.7 Hz, 1H), 3.92 (d, $^3J_{HH} = 2.7$ Hz, 1H), 4.46 (d, $^3J_{HH} = 4.1$ Hz, 1H), 6.89–7.02 (m, 4H), 7.10–7.16 (m, 2H), 7.20 (s, 2H), 7.65 (d, $^3J_{HH} = 7.5$ Hz, 1H), 7.89 (d, $^3J_{HH} = 7.5$ Hz, 1H); ^{13}C{^{1}H} NMR (100 MHz, C_6D_6, r.t.): δ 1.84 (CH_3), 1.89 (CH_3), 5.63 (CH_3), 22.65, 34.11 (CH), 38.13 (CH), 42.48 (d, $^2J_{CP} = 26.4$ Hz, CH), 46.94 (CH), 56.68 (d, $^1J_{CP} = 63.5$ Hz), 118.29, 118.98, 125.19 (CH), 126.19 (br, CH), 126.24 (CH), 126.43 (br d, $^3J_{CP} = 26.4$ Hz, CH), 127.06 (CH), 127.67 (CH), 127.71 (CH × 2), 128.20 (CH), 133.74 (d, $^1J_{CP} = 30.5$ Hz), 139.65, 140.17, 140.42 (d, $^2J_{CP} = 9.1$ Hz), 142.62, 146.40, 147.79; ^{31}P NMR (121 MHz, C_6D_6, r.t.): δ 518.8, 579.4 (AB quartet, $^1J_{PP} = 592$ Hz); HRMS (FAB) m/z, found: 941.4102 ([M + H]$^+$), calcd for $C_{48}H_{79}N_2P_2Si_7$ ([M + H]$^+$): 941.4103. Anal. Found: C, 61.07; H, 8.36; N, 3.07%. Calcd for $C_{48}H_{78}N_2P_2Si_7$: C, 61.22; H, 8.35; N, 2.97%. UV–vis (hexane): λ_{max} 490 (ε 450), 369 (1900), 317 nm (7700).

Reaction of BbtP=P(9-Anth) (1b) with 30 equiv of Maleonitrile (30d). A C_6D_6 suspension (0.9 mL) of

BbtP=P(9-Anth) (**1b**, 51.8 mg, 60.0 μmol) and maleonitrile (**30d**, 141 mg, 1.81 mmol) was degassed and sealed in an NMR tube. After heating at 120 °C for 12 h, the starting material **1b** and maleonitrile adduct **31d** were observed in the ratio of 3:97 as judged by the ^{1}H NMR spectra together with trace amount of **31c** and fumaronitrile (**30c**).[67] The reaction mixture was separated by GPLC and then PTLC (eluent: benzene, $R_f = 0.4$) to afford maleonitrile adduct **31d** (40.2 mg, 42.7 μmol, 71%). **31d**: orange crystals, mp: 215 °C (decomp.). ^{1}H NMR (400 MHz, C_6D_6, r.t.): δ 0.35 (s, 18H), 0.37 (s, 18H), 0.44 (s, 27H), 2.29 (dd, $^3J_{HH} = 9.7$, 2.2 Hz, 1H), 2.65 (s, 2H), 3.98 (d, $^3J_{HH} = 2.2$ Hz, 1H), 4.11 (d, $^3J_{HH} = 9.7$ Hz, 1H), 6.83 (dd, $^3J_{HH} = 7.3$ Hz, $^4J_{HH} = 1.2$ Hz, 1H), 6.88–6.93 (m, 2H), 6.96 (ddd, $^3J_{HH} = 7.5$, 7.3 Hz, $^4J_{HH} = 1.5$ Hz, 1H), 7.08 (ddd, $^3J_{HH} = 7.8$, 7.5 Hz, $^4J_{HH} = 1.2$ Hz, 1H), 7.18 (dd, $^3J_{HH} = 7.0$ Hz, $^4J_{HH} = 1.5$ Hz, 1H), 7.23 (s, 2H), 7.57 (d, $^3J_{HH} = 7.8$ Hz, 1H), 7.86 (d, $^3J_{HH} = 7.3$ Hz, 1H); ^{13}C{^{1}H} NMR (100 MHz, C_6D_6, r.t.): δ 1.83 (CH_3), 1.90 (CH_3), 5.66 (CH_3), 22.71, 34.06 (CH), 36.64 (CH), 41.02 (CH, d, $^2J_{CP} = 26.4$ Hz), 47.18 (CH), 56.70 (d, $^1J_{CP} = 61.0$ Hz), 117.31, 117.73, 124.65 (CH), 126.14 (br d, $^3J_{CP} = 23.9$ Hz, CH), 126.37 (CH), 126.43 (br, CH), 126.68 (CH), 127.70 (CH), 127.78 (CH), 127.82 (CH), 128.07 (CH), 133.80 (d, $^1J_{CP} = 33.0$ Hz), 138.61, 140.59 (d, $^2J_{CP} = 4.9$ Hz), 141.53, 142.67, 146.36, 147.84; ^{31}P NMR (121 MHz, C_6D_6, r.t.): δ 522.6, 578.3 (AB quartet, $^1J_{PP} = 592$ Hz). HRMS (FAB) m/z, found: 941.4092 ($[M + H]^+$), calcd for $C_{48}H_{79}N_2P_2Si_7$ ($[M + H]^+$): 941.4103. Anal. Found: C, 61.11; H, 8.37; N, 3.06%. Calcd for $C_{48}H_{78}N_2P_2Si_7$: C, 61.22; H, 8.35; N, 2.97%. UV–vis (hexane): λ_{max} 491 (ε 450), 366 (1800), 317 nm (7700).

Reaction of BbtP=P(9-Anth) (1b) with 5 equiv of Fumaronitrile (30c). A C_6D_6 suspension (0.9 mL) of BbtP=P(9-Anth) (**1b**, 51.8 mg, 60.0 μmol) and fumaronitrile (**30c**, 23.4 mg, 0.300 mmol) was degassed and sealed in an NMR tube. After heating at 120 °C for 72 h, the starting material **1b**, fumaronitrile adduct **31c**, and maleonitrile adduct **31d** were observed in the ratio of 14:63:23 as judged by the ^{1}H NMR spectra together with maleonitrile (**30d**).[67] The reaction mixture was separated by GPLC and then PTLC (eluent: benzene) to afford fumaronitrile adduct **31c** (25.1 mg, 26.6 μmol, 44%) and maleonitrile adduct **31d** (8.4 mg, 8.9 μmol, 15%) as orange crystals, respectively.

Reaction of Anthracene with 5 equiv of Fumaronitrile (30c). A C_6D_6 suspension (0.9 mL) of anthracene (10.7 mg, 60.0 μmol) and fumaronitrile (**30c**, 23.4 mg, 0.300 mmol) was degassed and sealed in an NMR tube. After heating at 120 °C for 24 h, the signals of anthracene disappeared as judged by the ^{1}H NMR spectra. No change was observed by ^{1}H NMR spectra after the additional heating at 120 °C for 48 h. The unreacted fumaronitrile and the solvent of the reaction mixture were removed under reduced pressure to afford the corresponding [4 + 2] cycloadduct of fumaronitrile (15.6 mg, 60 μmol, >99%). Data: colorless solids, mp: 194 °C (sublimed; lit.[68a] 274 °C, lit.[68b] 259 °C, lit.[68c] 259–260 °C). ^{1}H NMR (400 MHz, $CDCl_3$, r.t.): δ 3.13–3.14 (m, 2H), 4.64 (m, 2H), 7.23–7.30 (m, 4H), 7.34–7.38 (m, 2H), 7.44–7.47 (m, 2H); ^{13}C{^{1}H} NMR (75 MHz, $CDCl_3$, r.t.): δ 35.47 (CH), 46.32 (CH), 118.47, 124.16 (CH), 125.75 (CH), 127.82 (CH), 127.91 (CH), 137.33, 139.27. HRMS (EI) m/z, found: 256.0996 ($[M]^+$), calcd for $C_{18}H_{12}N_2$ ($[M]^+$): 256.1000. Anal. Found: C, 84.43; H, 4.84; N, 10.83%. Calcd for $C_{18}H_{12}N_2$: C, 84.35; H, 4.72; N, 10.93%.

Thermal Reaction of Fumaronitrile (30c): A C_6D_6 solution (0.75 mL) of fumaronitrile (**30c**, 15.6 mg, 0.20 mmol) was degassed and sealed in an NMR tube. After heating at 120 °C for 60 h, no change was observed by ^{1}H NMR spectrum.

Isomerization of Fumaronitrile (30c) into Maleonitrile (30d) in the Presence of Diphosphene (BbtP=PBbt): A C_6D_6 solution (0.6 mL) of BbtP=PBbt (6.6 mg, 5.0 μmol) and fumaronitrile (**30c**, 11.7 mg, 0.150 mmol) was degassed and sealed in an NMR tube. After heating at 120 °C for 24 h, fumaronitrile (**30c**) and maleonitirile (**30d**) were observed in the ratio of 68:32 as judged by ^{1}H NMR spectrum.

Thermal Reactions of [4 + 2] Cycloadducts 31a, 31c, and 31d in the Presence of *N*-Phenylmaleimide: A C_6D_6 solution (0.7 mL) of [4 + 2] cycloadduct **31** (7.2 μmol) and *N*-phenylmaleimide (**30b**, 12.5 mg, 72.2 μmol) was degassed and sealed in an NMR tube, and then heated at 120 °C for 24 h.

With maleic anhydride adduct **31a** (6.9 mg), the signals for **31a**, maleimide adduct **31b** generated from the [4 + 2] cycloaddition of anthryldiphosphene **1b** and **30b**, and the dissociated olefin **30a** was observed in the ratio of 88/12/4 (**31a**/**31b**/**30a**).

With fumaronitrile adduct **31c** (6.8 mg), the signals for **31c**, maleimide adduct **31b**, and the dissociated olefin **30c** was observed in the ratio of 83/17/4 (**31c**/**31b**/**30c**).

With maleonitrile adduct **31d** (6.8 mg), the signals for **31d**, maleimide adduct **31b**, and the dissociated olefin **30d** was observed in the ratio of 63/37/18 (**31d**/**31b**/**30d**).

X-ray Crystallographic Analysis of [2a·toluene], [2a·2(benzene)], [2b·benzene], 13, 14, 15, and 29. Crystal data for **1a**,[16] **1b**,[17] **20**,[18] and **31a**–**31d**[17] have been previously reported. Single crystals of **[2a·toluene]**, **[2a·2(benzene)]**, **[2b·benzene]**, **13**, **14**, **15**, and **29** were grown by slow recrystallization of their solution (toluene at −40 °C for **[2a·toluene]**, THF/benzene at room temperature for **[2a·2(benzene)]**, **[2b·benzene]**, and **15**, and toluene at room temperature for **13** and **14**) in a glovebox filled with argon or by slow recrystallization of its hexane solution at room temperature for **29** in a degassed and sealed tube, respectively. The intensity data were collected on a Rigaku Saturn70 CCD system with VariMax Mo Optic using Mo Kα radiation ($\lambda = 0.71070$ Å) for **[2a·toluene]**, **[2a·2(benzene)]**, **13**, and **15** or on a Rigaku Mercury CCD diffractometer with graphite-monochromated Mo Kα radiation ($\lambda = 0.71070$ Å) for **[2b·benzene]**, **14**, and **29**). Crystal data of **[2a·toluene]**, **[2a·2(benzene)]**, **[2b·benzene]**, **13**, **14**, **15**, and **29** are shown in Tables 8 and 9. The structure was solved by direct method (SIR-97[69] or SHELXS-97[70,71]) and refined by full-matrix least-squares procedures on F^2 for all reflections (SHELXL-97[71]). All hydrogen atoms were placed using AFIX instructions, while all the other atoms were refined anisotropically. The toluene molecule of **[2a·toluene]** was disordered and restrained using SADI instructions and refined isotropically. The benzene molecules of **[2a·2(benzene)]** were disordered and their occupancies were refined (0.70:0.30). One of the $SiMe_3$ groups at the *para*-position of the Bbt group of **[2b·benzene]** was disordered and their occupancies were refined (0.60:0.40). The $SiMe_3$ group at the *para*-position of the Bbt group of **29** was disordered and their

Table 8. Crystal Data for **[2a·toluene]**, **[2a·2(benzene)]**, and **[2b·benzene]**

	[2a·toluene]	**[2a·2(benzene)]**	**[2b·benzene]**
Formula	$C_{75}H_{134}P_4Si_{12}$	$C_{80}H_{138}P_4Si_{12}$	$C_{80}H_{148}P_4Si_{14}$
Formula weight	1496.78	1560.86	1627.12
Crystal dimensions/mm^3	0.12 × 0.07 × 0.01	0.20 × 0.10 × 0.02	0.30 × 0.25 × 0.20
Temperature/K	103(2)	103(2)	103(2)
Crystal system	triclinic	triclinic	monoclinic
Space group	$P\bar{1}$ (#2)	$P\bar{1}$ (#2)	$P2_1/n$ (#14)
Lattice parameters			
a/Å	12.8565(4)	11.3090(4)	13.7457(5)
b/Å	18.2969(3)	12.9678(6)	21.6626(14)
c/Å	22.8753(6)	17.4048(6)	17.7072(7)
α/°	114.1033(13)	80.4087(17)	90
β/°	101.2683(16)	70.9895(15)	110.0132(16)
γ/°	89.589(2)	80.9990(14)	90
V/Å^3	4801.3(2)	2365.18(16)	4954.2(4)
Z	2	1	2
D_{calcd}/g cm^{-3}	1.035	1.096	1.091
μ/mm^{-1}	0.263	0.269	0.282
$2\theta_{max}$/°	51	51	51
No. of reflections	50895	21031	43114
Independent reflections	17635	8747	9217
No. of parameters	841	482	479
R_{int}	0.0465	0.0690	0.0501
Completeness to θ/%	98.5	99.3	99.8
R_1 [$I > 2\sigma(I)$]	0.0559	0.0579	0.0590
wR_2 (all data)	0.1564	0.1457	0.1534
Largest diff. peak/e.Å^{-3}	0.814	0.657	0.734
Largest diff. hole/e.Å^{-3}	−0.456	−0.738	−0.949
Goodness-of-fit	1.038	1.030	1.027

Table 9. Crystal Data for **13**, **14**, **15**, and **29**

	13	**14**	**15**	**29**
Formula	$C_{46}H_{68}CrO_5P_2Si_6$	$C_{44}H_{76}P_2SSi_7$	$C_{44}H_{76}P_2SeSi_7$	$C_{50}H_{86}P_2Si_7$
Formula weight	983.48	895.68	942.58	945.76
Crystal dimensions/mm^3	0.12 × 0.10 × 0.01	0.30 × 0.15 × 0.10	0.08 × 0.05 × 0.01	0.20 × 0.10 × 0.10
Temperature/K	103(2)	103(2)	103(2)	103(2)
Crystal system	monoclinic	triclinic	triclinic	triclinic
Space group	$P2_1/n$ (#14)	$P\bar{1}$ (#2)	$P\bar{1}$ (#2)	$P\bar{1}$ (#2)
Lattice parameters				
a/Å	14.5601(2)	9.1987(11)	9.2554(2)	9.7559(4)
b/Å	24.8189(3)	12.8602(17)	12.9484(2)	15.2253(4)
c/Å	16.1422(2)	24.446(4)	22.7049(4)	19.4232(10)
α/°	90	75.796(9)	79.0674(9)	84.872(5)
β/°	112.9695(5)	78.454(6)	85.2365(8)	88.670(6)
γ/°	90	69.799(5)	81.1160(12)	82.224(6)
V/Å^3	5370.73(12)	2609.7(6)	2635.52(8)	2846.9(2)
Z	4	2	2	2
D_{calcd}/g cm^{-3}	1.216	1.140	1.188	1.103
μ/mm^{-1}	0.446	0.312	0.960	0.254
$2\theta_{max}$/°	51	51	51	51
No. of reflections	47458	22005	23573	24920
Independent reflections	9997	9468	9765	10482
No. of parameters	559	584	508	574
R_{int}	0.0930	0.0813	0.0323	0.0344
Completeness to θ/%	100.0	97.5	99.4	98.9
R_1 [$I > 2\sigma(I)$]	0.0441	0.0697	0.0353	0.0461
wR_2 (all data)	0.0970	0.2015	0.0891	0.1126
Largest diff. peak/e.Å^{-3}	0.438	0.686	0.761	0.379
Largest diff. hole/e.Å^{-3}	−0.300	−0.377	−0.346	−0.340
Goodness-of-fit	1.052	1.002	1.040	1.082

occupancies were refined (0.92:0.08). Crystallographic data for the structure reported in this paper have been deposited with Cambridge Crystallographic Data Centra as supplementary publication Nos. CCDC 753012 for **[2a·toluene]**, CCDC 753011 for **[2a·2(benzene)]**, CCDC 753013 for **[2b·benzene]**, CCDC 753007 for **13**, CCDC 753008 for **14**, CCDC 753009 for **15**, and CCDC 753010 for **29**. Copies of the data can be obtained free of charge on application to CCDC, 12, Union Road, Cambridge, CB2 1EZ, U.K. (fax: +44 1223 336033; E-mail: deposit@ccdc.cam.ac.uk.).

Measurement of Fluorescence Spectra of 1a, 2a, 2b, and 13. Fluorescence and excitation spectra of **1a**, **2a**, **2b**, and **13** were measured at room temperature under the condisions as follows: **1a**; Excitation wavelength for fluorescence spectra, $\lambda_{ex} = 400$ or 530 nm; Observation wavelength for excitation spectra, $\lambda_{em} = 432$ nm. **2a**; Excitation wavelength for fluorescence spectra, $\lambda_{ex} = 426$ or 538 nm. **2b**; Excitation wavelength for fluorescence spectra, $\lambda_{ex} = 427$ or 542 nm; **13**; Excitation wavelength for fluorescence spectra, $\lambda_{ex} = 400$ or 465 nm.

Measurement of Lifetime of the Photoluminescence of 1a. In a glovebox filled with argon, **1** was dissolved in hexane (distilled over K mirror and then distilled by trap-to-trap). This solution (1.3×10^{-5} M) was put into a quartz cell (pathlength 1.0 cm). The fluorescent cell was degassed and sealed. Lifetime of the photoluminescence was measured under the following conditions: Excitation wavelength, $\lambda_{ex} = 400$ with filter L42 (which cut under 420 nm); Slit width, 500 μm; Time range, 50 ns; Measure times, 10000 times.

Theoretical Calculations. All theoretical calculations were carried out using the Gaussian 98[72] or 03[73] series of electronic structure programs with density functional theory at B3LYP level.[74] The optimized structures of **8**, [$\mathbf{8}^{\bullet-}$], **9**, and [$\mathbf{9}^{\bullet-}$] and TDDFT calculations of **8** have been previously reported.[15] The geometries were optimized by using B3LYP/6-31G(d) level (for *syn*-**2a** and *anti*-**2a**), B3LYP/6-31G(d) for C, H and 6-311+G(2d) for P level (for *syn*-**12** and *anti*-**12**), B3LYP/6-31G(d) for C, H and TZ(2d) for P, Se (for **18** and **19**), and B3LYP/6-31G(d) for C, H, O and 6-311+G(2d) for P level (for **33a**). It was confirmed that the optimized structures have minimum energies by frequency calculations. The TDDFT calculations of *syn*-**12**, *anti*-**12**, and **33a** were performed at 6-31+G(2d,p) level. The GIAO calculations of **18** and **19** were performed at 6-311+G(2d,p) level. Theoretically optimized coordinates of *syn*-**2a**, *anti*-**2a**, *syn*-**12**, *anti*-**12**, **18**, **19**, and **33a** are shown in Supporting Information, and selected molecular orbitals of **8**, *syn*-**12**, *anti*-**12**, and **33a** are shown in Figure 10, Figures S1–S3, respectively.

This work was supported by Grants-in-Aid for Creative Scientific Research (No. 17GS0207), Science Research on Priority Areas (No. 20036024, "Synergy of Elements"), and the Global COE Program ("Integrated Materials Science"), Kyoto University from the Ministry of Education, Culture, Sports, Science and Technology, Japan. A. T. is grateful for a JSPS fellowship for young scientists.

Supporting Information

Theoretically optimized coordinates of all calculated compounds and selected molecular orbitals of *syn*-**12**, *anti*-**12**, and **33a**. This material is available free of charge on the web at http://www.csj.jp/journals/bcsj/.

References

1 For reviews, see: a) L. Weber, *Chem. Rev.* **1992**, *92*, 1839. b) P. P. Power, *Chem. Rev.* **1999**, *99*, 3463. c) N. Tokitoh, *J. Organomet. Chem.* **2000**, *611*, 217. d) P. P. Power, *J. Organomet. Chem.* **2004**, *689*, 3904. e) T. Sasamori, N. Tokitoh, *Dalton Trans.* **2008**, 1395.

2 M. Yoshifuji, I. Shima, N. Inamoto, K. Hirotsu, T. Higuchi, *J. Am. Chem. Soc.* **1981**, *103*, 4587.

3 For examples, see: a) A. H. Cowley, J. G. Lasch, N. C. Norman, M. Pakulski, *J. Am. Chem. Soc.* **1983**, *105*, 5506. b) B. Twamley, C. D. Sofield, M. M. Olmstead, P. P. Power, *J. Am. Chem. Soc.* **1999**, *121*, 3357. c) A. H. Cowley, J. G. Lasch, N. C. Norman, M. Pakulski, B. R. Whittlesey, *J. Chem. Soc., Chem. Commun.* **1983**, 881. d) B. Twamley, P. P. Power, *Chem. Commun.* **1998**, 1979.

4 For examples, see: a) N. Tokitoh, Y. Arai, T. Sasamori, R. Okazaki, S. Nagase, H. Uekusa, Y. Ohashi, *J. Am. Chem. Soc.* **1998**, *120*, 433. b) N. Tokitoh, Y. Arai, R. Okazaki, S. Nagase, *Science* **1997**, *277*, 78. c) T. Sasamori, Y. Arai, N. Takeda, R. Okazaki, Y. Furukawa, M. Kimura, S. Nagase, N. Tokitoh, *Bull. Chem. Soc. Jpn.* **2002**, *75*, 661. d) T. Sasamori, N. Takeda, M. Fujio, M. Kimura, S. Nagase, N. Tokitoh, *Angew. Chem., Int. Ed.* **2002**, *41*, 139. e) T. Sasamori, N. Takeda, N. Tokitoh, *Chem. Commun.* **2000**, 1353. f) T. Sasamori, N. Takeda, N. Tokitoh, *J. Phys. Org. Chem.* **2003**, *16*, 450.

5 a) T. Sasamori, E. Mieda, N. Nagahora, N. Takeda, N. Takagi, S. Nagase, N. Tokitoh, *Chem. Lett.* **2005**, *34*, 166. b) T. Sasamori, E. Mieda, N. Nagahora, K. Sato, D. Shiomi, T. Takui, Y. Hosoi, Y. Furukawa, N. Takagi, S. Nagase, N. Tokitoh, *J. Am. Chem. Soc.* **2006**, *128*, 12582. c) N. Nagahora, T. Sasamori, Y. Hosoi, Y. Furukawa, N. Tokitoh, *J. Organomet. Chem.* **2008**, *693*, 625.

6 For examples, see: a) R. Gleiter, G. Friedrich, M. Yoshifuji, K. Shibayama, N. Inamoto, *Chem. Lett.* **1984**, 313. b) S. Elbel, A. Ellis, E. Niecke, H. Egsgaard, L. Carlsen, *J. Chem. Soc., Dalton Trans.* **1985**, 879. c) T. L. Allen, A. C. Scheiner, Y. Yamaguchi, H. F. Schaefer, III, *J. Am. Chem. Soc.* **1986**, *108*, 7579. d) K. Ito, S. Nagase, *Chem. Phys. Lett.* **1986**, *126*, 531. e) S. Nagase, S. Suzuki, T. Kurakake, *J. Chem. Soc., Chem. Commun.* **1990**, 1724. f) T. L. Allen, A. C. Scheiner, H. F. Schaefer, III, *J. Phys. Chem.* **1990**, *94*, 7780. g) A. H. Cowley, A. Decken, N. C. Norman, C. Krüger, F. Lutz, H. Jacobsen, T. Ziegler, *J. Am. Chem. Soc.* **1997**, *119*, 3389. h) K. Miqueu, J.-M. Sotiropoulos, G. Pfister-Guillouzo, H. Ranaivonjatovo, J. Escudié, *J. Mol. Struct.* **2001**, *595*, 139. i) H.-L. Peng, J. L. Payton, J. D. Protasiewicz, M. C. Simpson, *J. Phys. Chem. A* **2009**, *113*, 7054.

7 a) B. Cetinkaya, P. B. Hitchcock, M. F. Lappert, A. J. Thorne, H. Goldwhite, *J. Chem. Soc., Chem. Commun.* **1982**, 691. b) M. Culcasi, G. Gronchi, J. Escudié, C. Couret, L. Pujol, P. Tordo, *J. Am. Chem. Soc.* **1986**, *108*, 3130. c) A. J. Bard, A. H. Cowley, J. E. Kilduff, J. K. Leland, N. C. Norman, M. Pakulski, G. A. Heath, *J. Chem. Soc., Dalton Trans.* **1987**, 249. d) H. Binder, B. Riegel, G. Heckmann, M. Moscherosch, W. Kaim, H.-G. von Schnering, W. Hönle, H.-J. Flad, A. Savin, *Inorg. Chem.* **1996**, *35*, 2119. e) S. Shah, S. C. Burdette, S. Swavey, F. L. Urbach, J. D. Protasiewicz, *Organometallics* **1997**, *16*, 3395. f) J. Geier, J. Harmer, H. Grützmacher, *Angew. Chem., Int. Ed.* **2004**, *43*, 4093.

8 For a review, see: T. Baumgartner, R. Réau, *Chem. Rev.*

2006, *106*, 4681.

9 It is predicted that a phosphorus atom has considerable conjugative ability similar to a carbon atom in olefin-like compounds such as phosphaalkene (P=C) and diphosphene (P=P) due to the similar electronegativity (P, 2.2; C, 2.5), see also: a) *Phosphorus: The Carbon Copy: From Organophosphorus to Phospha-organic Chemistry*; ed. by K. B. Dillon, F. Mathey, J. F. Nixon, John Wiley & Sons, New York, **1998**. b) L. Nyulászi, T. Veszprémi, J. Réffy, *J. Phys. Chem.* **1993**, *97*, 4011.

10 a) K. Tsuji, S. Sasaki, M. Yoshifuji, *Tetrahedron Lett.* **1999**, *40*, 3203. b) S. Sasaki, H. Aoki, K. Sutoh, S. Hakiri, K. Tsuji, M. Yoshifuji, *Helv. Chim. Acta* **2002**, *85*, 3842. c) S. Kawasaki, A. Nakamura, K. Toyota, M. Yoshifuji, *Bull. Chem. Soc. Jpn.* **2005**, *78*, 1110.

11 a) V. A. Wright, D. P. Gates, *Angew. Chem., Int. Ed.* **2002**, *41*, 2389. b) R. C. Smith, X. Chen, J. D. Protasiewicz, *Inorg. Chem.* **2003**, *42*, 5468. c) R. C. Smith, J. D. Protasiewicz, *J. Am. Chem. Soc.* **2004**, *126*, 2268. d) R. C. Smith, J. D. Protasiewicz, *Eur. J. Inorg. Chem.* **2004**, 998. e) S. Shah, T. Concolino, A. L. Rheingold, J. D. Protasiewicz, *Inorg. Chem.* **2000**, *39*, 3860. f) C. Dutan, S. Shah, R. C. Smith, S. Choua, T. Berclaz, M. Geoffroy, J. D. Protasiewicz, *Inorg. Chem.* **2003**, *42*, 6241. g) V. A. Wright, B. O. Patrick, C. Schneider, D. P. Gates, *J. Am. Chem. Soc.* **2006**, *128*, 8836.

12 a) S. Shah, J. D. Protasiewicz, *Chem. Commun.* **1998**, 1585. b) R. Pietschnig, E. Niecke, *Organometallics* **1996**, *15*, 891. c) C. Moser, A. Orthaber, M. Nieger, F. Belaj, R. Pietschnig, *Dalton Trans.* **2006**, 3879. d) C. Moser, M. Nieger, R. Pietschnig, *Organometallics* **2006**, *25*, 2667. e) N. Nagahora, T. Sasamori, N. Takeda, N. Tokitoh, *Chem.—Eur. J.* **2004**, *10*, 6146. f) N. Nagahora, T. Sasamori, N. Takeda, N. Tokitoh, *Organometallics* **2005**, *24*, 3074. g) N. Nagahora, T. Sasamori, N. Tokitoh, *Chem. Lett.* **2006**, *35*, 220. h) N. Nagahora, T. Sasamori, Y. Watanabe, Y. Furukawa, N. Tokitoh, *Bull. Chem. Soc. Jpn.* **2007**, *80*, 1884. i) N. Nagahora, T. Sasamori, N. Tokitoh, *Organometallics* **2008**, *27*, 4265.

13 a) B. Schäfer, E. Öberg, M. Kritikos, S. Ott, *Angew. Chem., Int. Ed.* **2008**, *47*, 8228. b) X.-L. Geng, S. Ott, *Chem. Commun.* **2009**, 7206.

14 M. Yoshifuji, N. Shinohara, K. Toyota, *Tetrahedron Lett.* **1996**, *37*, 7815.

15 a) A. Jouaiti, A. Al Badri, M. Geoffroy, G. Bernardinelli, *J. Organomet. Chem.* **1997**, *529*, 143. b) S. Shah, J. D. Protasiewicz, *Coord. Chem. Rev.* **2000**, *210*, 181. c) F. Murakami, S. Sasaki, M. Yoshifuji, *J. Am. Chem. Soc.* **2005**, *127*, 8926.

16 T. Sasamori, A. Tsurusaki, N. Nagahora, K. Matsuda, Y. Kanemitsu, Y. Watanabe, Y. Furukawa, N. Tokitoh, *Chem. Lett.* **2006**, *35*, 1382.

17 A. Tsurusaki, T. Sasamori, N. Tokitoh, *Organometallics* **2009**, *28*, 3604.

18 Tellurization reaction of 9-anthryldiphosphene **1b** has already been reported, see: N. Tokitoh, A. Tsurusaki, T. Sasamori, *Phosphorus, Sulfur Silicon Relat. Elem.* **2009**, *184*, 979.

19 [4 + 2] Cycloaddition reaction of 9-anthryldiphosphene **1b** has been preliminarily reported, see Ref. 17.

20 M. Yoshifuji, K. Shibayama, N. Inamoto, T. Matsushita, K. Nishimoto, *J. Am. Chem. Soc.* **1983**, *105*, 2495.

21 Slow addition of dilute, not neat DBU is necessary to increase the yield.

22 For example, Mes*P=PMes was reported to show the AB quartet signals at δ 467.6 and 540.4 with $^1J_{PP} = 573.7$ Hz, see Ref. 20.

23 The theoretically optimized parameters for s*yn*-**2a** and *anti*-**2a** are comparable to those experimentally observed for *syn*-**2a**, *anti*-**2a**, and *anti*-**2b**.

24 a) H. Hamaguchi, M. Tasumi, M. Yoshifuji, N. Inamoto, *J. Am. Chem. Soc.* **1984**, *106*, 508. b) T. Copeland, M. P. Shea, M. C. Milliken, R. C. Smith, J. D. Protasiewicz, M. C. Simpson, *Anal. Chim. Acta* **2003**, *496*, 155. c) V. Cappello, J. Baumgartner, A. Dransfeld, M. Flock, K. Hassler, *Eur. J. Inorg. Chem.* **2006**, 2393.

25 K. Hassler, F. Höfler, *Z. Anorg. Allg. Chem.* **1978**, *443*, 125.

26 The theoretically calculated frequiencies are scaled by 0.96, see: a) M. W. Wong, *Chem. Phys. Lett.* **1996**, *256*, 391. b) A. P. Scott, L. Radom, *J. Phys. Chem.* **1996**, *100*, 16502. c) C. W. Bauschlicher, Jr., H. Partridge, *J. Chem. Phys.* **1995**, *103*, 1788. d) H. Yoshida, H. Matsuura, *J. Phys. Chem. A* **1998**, *102*, 2691.

27 In some cases, a Bbt-substituted compound has relatively high solubility compared to that of a Tbt-substituted one. For example, ArE=EAr (E = Sb, Bi, Ar = Tbt or Bbt); see Ref. 4c.

28 Very recently, an anthryldisilene was reported to show similar communication between the anthryl and Si=Si units in the UV–vis spectrum. The absorption at longer wavelength was assigned to the π(Si=Si)–π^*(9-Anth) transitions, see: T. Iwamoto, M. Kobayashi, K. Uchiyama, S. Sasaki, S. Nagendran, H. Isobe, M. Kira, *J. Am. Chem. Soc.* **2009**, *131*, 3156.

29 A. Tsurusaki, T. Sasamori, N. Nagahora, N. Tokitoh, unpublished results.

30 W. H. Melhuish, *J. Phys. Chem.* **1961**, *65*, 229.

31 It has been reported that Ph_2(9-Anth)P and (9-Anth)$_3$P show no fluorescence, whereas the corresponding phosphine oxides exhibit intense fluorescence, see: a) S. Yamaguchi, S. Akiyama, K. Tamao, *J. Organomet. Chem.* **2002**, *652*, 3. b) S. Yamaguchi, S. Akiyama, K. Tamao, *J. Organomet. Chem.* **2002**, *646*, 277. c) K. Akasaka, T. Suzuki, H. Ohrui, H. Meguro, *Anal. Lett.* **1987**, *20*, 731.

32 W. R. Ware, B. A. Baldwin, *J. Chem. Phys.* **1965**, *43*, 1194.

33 Z. Fei, N. Kocher, C. J. Mohrschladt, H. Ihmels, D. Stalke, *Angew. Chem., Int. Ed.* **2003**, *42*, 783.

34 a) J. H. K. Yip, J. Prabhavathy, *Angew. Chem., Int. Ed.* **2001**, *40*, 2159. b) R. Lin, J. H. K. Yip, K. Zhang, L. L. Koh, K.-Y. Wong, K. P. Ho, *J. Am. Chem. Soc.* **2004**, *126*, 15852.

35 Diphosphene oxide (Mes*P=P(=O)Mes*) is postulated as a reactive intermediate in the oxidation reaction of Mes*P=PMes* with *m*-chloroperbenzoic acid (*m*CPBA) or photochemical oxidation reaction, see: a) M. Yoshifuji, K. Shibayama, I. Shima, N. Inamoto, *Phosphorus, Sulfur Silicon Relat. Elem.* **1983**, *18*, 11. b) M. Yoshifuji, K. Ando, K. Toyota, I. Shima, N. Inamoto, *J. Chem. Soc., Chem. Commun.* **1983**, 419. c) A. M. Caminade, F. E. Khatib, C. Ades, M. Verrier, N. Paillous, M. Koenig, *Phosphorus, Sulfur Silicon Relat. Elem.* **1986**, *26*, 91.

36 The reaction of the diphosphene (Mes*P=PMes*) with an excess amount of [Et$_3$PAu][PF$_6$] has been reported to give a monocationic species of diphosphene. Only the ^{31}P spectral data of this compound was reported, see: A. H. Cowley, N. C. Norman, M. Pakulski, *J. Chem. Soc., Chem. Commun.* **1984**, 1054.

37 D. V. Partyka, M. P. Washington, T. G. Gray, J. B. Updegraff, III, J. F. Turner, II, J. D. Protasiewicz, *J. Am. Chem. Soc.* **2009**, *131*, 10041.

38 M. Yoshifuji, *Bull. Chem. Soc. Jpn.* **1997**, *70*, 2881.

39 a) M. Yoshifuji, T. Hashida, N. Inamoto, K. Hirotsu, T. Horiuchi, T. Higuchi, K. Ito, S. Nagase, *Angew. Chem., Int. Ed. Engl.* **1985**, *24*, 211. b) M. Yoshifuji, T. Hashida, K. Shibayama, N. Inamoto, *Chem. Lett.* **1985**, 287.

40 a) J. Borm, L. Zsolnai, G. Huttner, *Angew. Chem., Int. Ed.*

Engl. **1983**, *22*, 977. b) K. M. Flynn, H. Hope, B. D. Murray, M. M. Olmstead, P. P. Power, *J. Am. Chem. Soc.* **1983**, *105*, 7750. c) A.-M. Hinke, A. Hinke, W. Kuchen, W. Hönle, *Z. Naturforsch. B* **1986**, *41*, 629. d) R. A. Barlett, H. V. R. Dias, K. M. Flynn, H. Hope, B. D. Murray, M. M. Olmstead, P. P. Power, *J. Am. Chem. Soc.* **1987**, *109*, 5693.

41 The chromium complex bearing phosphinine ligands, $(\eta^1\text{-}C_5H_5P)_6Cr$, showed an MLCT absorption at longer wavelength due to the low-lying π^*-orbital of the phosphinine ligand, see: C. Elschenbroich, S. Voss, O. Schiemann, A. Lippek, K. Harms, *Organometallics* **1998**, *17*, 4417.

42 a) M. Yoshifuji, K. Shibayama, N. Inamoto, K. Hirotsu, T. Higuchi, *J. Chem. Soc., Chem. Commun.* **1983**, 862. b) M. Yoshifuji, K. Shibayama, N. Inamoto, *Heterocycles* **1984**, *22*, 681. c) M. Yoshifuji, D.-L. An, K. Toyota, M. Yasunami, *Chem. Lett.* **1993**, 2069. d) M. Yoshifuji, K. Ando, K. Shibayama, N. Inamoto, K. Hirotsu, T. Higuchi, *Angew. Chem., Int. Ed. Engl.* **1983**, *22*, 418.

43 a) M. Yoshifuji, K. Shibayama, N. Inamoto, *Chem. Lett.* **1984**, 603. b) H. Voelker, U. Pieper, H. W. Roesky, G. M. Sheldrick, *Z. Naturforsch. B* **1994**, *49*, 255. c) P. Jutzi, N. Brusdeilins, H.-G. Stammler, B. Neumann, *Chem. Ber.* **1994**, *127*, 997.

44 a) T. Sasamori, E. Mieda, N. Tokitoh, *Bull. Chem. Soc. Jpn.* **2007**, *80*, 2425. b) N. Nagahora, T. Sasamori, N. Tokitoh, *Heteroat. Chem.* **2008**, *19*, 443.

45 a) W.-W. du Mont, T. Severengiz, *Z. Anorg. Allg. Chem.* **1993**, *619*, 1083. b) W.-W. Du Mont, T. Severengiz, B. Meyer, *Angew. Chem., Int. Ed. Engl.* **1983**, *22*, 983. c) L. Weber, G. Meine, R. Boese, N. Niederprüm, *Z. Naturforsch. B* **1988**, *43*, 715.

46 Tributylphosphine telluride is known to work as a better tellurization reagent toward heavier dipnictenes than elemental tellurium, see: Ref. 44.

47 a) M. Baudler, K. Glinka, *Chem. Rev.* **1993**, *93*, 1623. b) A.-M. Caminade, J.-P. Majoral, R. Mathieu, *Chem. Rev.* **1991**, *91*, 575.

48 The molecular structure of triphosphirane **20** has already been reported, see: Ref. 18.

49 A. J. C. Wilson, International Tables for Crystallography, ed. by F. H. Allen, A. G. Orpen, R. Taylor, The International Union of Crystallography by Kluwer Academic Publishers, Dordrecht/Boston/London, **1992**, Vol. C, Chap. 9.5, pp. 685–706.

50 J. Emsley, *The Elements*, 3rd ed., Oxford University Press, New York, **1998**.

51 J. Escudié, C. Couret, J. D. Andriamizaka, J. Satgé, *J. Organomet. Chem.* **1982**, *228*, C76.

52 a) P. Jutzi, U. Meyer, B. Krebs, M. Dartmann, *Angew. Chem., Int. Ed. Engl.* **1986**, *25*, 919. b) V. D. Romanenko, E. O. Klebanskii, L. N. Markovskii, *Zh. Obshch. Khim.* **1986**, *56*, 2159. c) L. N. Markovskii, V. D. Romanenko, M. I. Povolotskii, A. V. Ruban, E. O. Klebanskii, *Zh. Obshch. Khim.* **1986**, *56*, 2157. d) L. N. Markovski, V. D. Romanenko, A. V. Ruban, *Phosphorus, Sulfur Silicon Relat. Elem.* **1987**, *30*, 447.

53 For a recent review, see: J. C. C. Atherton, S. Jones, *Tetrahedron* **2003**, *59*, 9039.

54 A few examples of diphosphenes have been reported to react with electron-deficient olefins to afford the corresponding [2 + 2] cycloadducts, see: a) L. Weber, M. Frebel, R. Boese, *Chem. Ber.* **1990**, *123*, 733. b) L. Weber, M. Frebel, A. Müller, H. Bögge, *Organometallics* **1991**, *10*, 1130.

55 Weber and co-workers have proposed the similar zwitterionic species as an intermediate by the [2 + 2] cycloaddition reaction of the diphosphene, $(\eta^5\text{-}C_5Me_5)(CO)_2FeP{=}PMes^*$ with dimethyl maleate or *N*-methylmaleimide, see: Ref. 54.

56 S. Loss, C. Widauer, H. Grützmacher, *Angew. Chem., Int. Ed.* **1999**, *38*, 3329.

57 The molecular orbitals of the model compound **33a** are shown in Supporting Information.

58 A. B. Pangborn, M. A. Giardello, R. H. Grubbs, R. K. Rosen, F. J. Timmers, *Organometallics* **1996**, *15*, 1518.

59 D. J. Dellinger, D. M. Sheehan, N. K. Christensen, J. G. Lindberg, M. H. Caruthers, *J. Am. Chem. Soc.* **2003**, *125*, 940.

60 a) R. A. Zingaro, B. H. Steeves, K. Irgolic, *J. Organomet. Chem.* **1965**, *4*, 320. b) L. Huang, R. A. Zingaro, E. A. Meyers, J. H. Reibenspies, *Heteroat. Chem.* **1996**, *7*, 57.

61 R. P. Linstead, M. Whalley, *J. Chem. Soc.* **1952**, 4839.

62 For the preparation of 9-lithioanthracene, see: a) L. Heuer, D. Schomburg, R. Schmutzler, *Chem. Ber.* **1989**, *122*, 1473. b) H.-D. Becker, L. Hansen, K. Andersson, *J. Org. Chem.* **1986**, *51*, 2956.

63 J. Wesemann, P. G. Jones, D. Schomburg, L. Heuer, R. Schmutzler, *Chem. Ber.* **1992**, *125*, 2187.

64 For the preparation of 9,10-dilithioanthracene, see: a) B. F. Duerr, Y.-S. Chung, A. W. Czarnik, *J. Org. Chem.* **1988**, *53*, 2120. b) Y. Chung, B. F. Duerr, T. A. McKelvey, P. Nanjappan, A. W. Czarnik, *J. Org. Chem.* **1989**, *54*, 1018. c) J. K. Kendall, H. Shechter, *J. Org. Chem.* **2001**, *66*, 6643.

65 C. Barré, P. Boudot, M. M. Kubicki, C. Moïse, *Inorg. Chem.* **1995**, *34*, 284.

66 The coupling constants were decided by the Water Eliminated FT (WEFT) method.

67 The ^{1}H NMR signals of **30c** ($\delta = 4.18$) and **30d** ($\delta = 4.06$) in C_6D_6 were identical to the corresponding signals (**30c** ($\delta = 6.27$) and **30d** ($\delta = 6.18$)) in $CDCl_3$, respectively. See: R. J. Halter, R. L. Fimmen, R. J. McMahon, S. A. Peebles, R. L. Kuczkowski, J. F. Stanton, *J. Am. Chem. Soc.* **2001**, *123*, 12353.

68 a) E. Weber, I. Csöregh, J. Ahrendt, S. Finge, M. Czugler, *J. Org. Chem.* **1988**, *53*, 5831. b) D. T. Mowry, *J. Am. Chem. Soc.* **1947**, *69*, 573. c) B. A. Arbuzov, A. N. Vereshchagin, *Izv. Akad. Nauk SSSR, Ser. Khim.* **1966**, *10*, 1731.

69 A. Altomare, M. C. Burla, M. Camalli, G. L. Cascarano, C. Giacovazzo, A. Guagliardi, A. G. G. Moliterni, G. Polidori, R. Spagna, *J. Appl. Cryst.* **1999**, *32*, 115.

70 G. M. Sheldrick, *Acta Crystallogr., Sect. A* **1990**, *46*, 467.

71 G. M. Sheldrick, *SHELX-97, Program for the Refinement of Crystal Structures*, University of Göttingen, Göttingen, Germany, **1997**.

72 M. J. Frisch, G. W. Trucks, H. B. Schlegel, G. E. Scuseria, M. A. Robb, J. R. Cheeseman, V. G. Zakrzewski, J. A. Montgomery, Jr., R. E. Stratmann, J. C. Burant, S. Dapprich, J. M. Millam, A. D. Daniels, K. N. Kudin, M. C. Strain, O. Farkas, J. Tomasi, V. Barone, M. Cossi, R. Cammi, B. Mennucci, C. Pomelli, C. Adamo, S. Clifford, J. Ochterski, G. A. Petersson, P. Y. Ayala, Q. Cui, K. Morokuma, P. Salvador, J. J. Dannenberg, D. K. Malick, A. D. Rabuck, K. Raghavachari, J. B. Foresman, J. Cioslowski, J. V. Ortiz, A. G. Baboul, B. B. Stefanov, G. Liu, A. Liashenko, P. Piskorz, I. Komaromi, R. Gomperts, R. L. Martin, D. J. Fox, T. Keith, M. A. Al-Laham, C. Y. Peng, A. Nanayakkara, M. Challacombe, P. M. W. Gill, B. Johnson, W. Chen, M. W. Wong, J. L. Andres, C. Gonzalez, M. Head-Gordon, E. S. Replogle, J. A. Pople, *Gaussian 98, Revision A.11*, Gaussian, Inc., Pittsburgh PA, **2001**.

73 M. J. Frisch, G. W. Trucks, H. B. Schlegel, G. E. Scuseria,

M. A. Robb, J. R. Cheeseman, J. A. Montgomery, Jr., T. Vreven, K. N. Kudin, J. C. Burant, J. M. Millam, S. S. Iyengar, J. Tomasi, V. Barone, B. Mennucci, M. Cossi, G. Scalmani, N. Rega, G. A. Petersson, H. Nakatsuji, M. Hada, M. Ehara, K. Toyota, R. Fukuda, J. Hasegawa, M. Ishida, T. Nakajima, Y. Honda, O. Kitao, H. Nakai, M. Klene, X. Li, J. E. Knox, H. P. Hratchian, J. B. Cross, C. Adamo, J. Jaramillo, R. Gomperts, R. E. Stratmann, O. Yazyev, A. J. Austin, R. Cammi, C. Pomelli, J. W. Ochterski, P. Y. Ayala, K. Morokuma, G. A. Voth, P. Salvador, J. J. Dannenberg, V. G. Zakrzewski, S. Dapprich, A. D. Daniels, M. C. Strain, O. Farkas, D. K. Malick, A. D. Rabuck, K. Raghavachari, J. B. Foresman, J. V. Ortiz, Q. Cui, A. G. Baboul, S. Clifford, J. Cioslowski, B. B. Stefanov, G. Liu, A. Liashenko, P. Piskorz, I. Komaromi, R. L. Martin, D. J. Fox, T. Keith, M. A. Al-Laham, C. Y. Peng, A. Nanayakkara, M. Challacombe, P. M. W. Gill, B. Johnson, W. Chen, M. W. Wong, C. Gonzalez, J. A. Pople, *Gaussian 03, Revision C.02*, Gaussian, Inc., Wallingford CT, **2004**.

74 a) C. Lee, W. Yang, R. G. Parr, *Phys. Rev. B* **1988**, *37*, 785. b) A. D. Becke, *J. Chem. Phys.* **1993**, *98*, 5648. c) A. D. Becke, *Phys. Rev. A* **1988**, *38*, 3098.